

Aerodynamics as the Basis of Aviation: How Well Did It Do?

J. A. D. Ackroyd
Timperley, Cheshire

In memory of the Royal Aircraft Establishment, its staff and contributions to aerodynamics

Abstract

The paper describes the role of aerodynamics in the enhancement of aeroplane performance. To illustrate this, drag and lift-to-drag data are reviewed, covering the first half-century of powered, controllable flight. The survey begins with the Wright Flyer and the biplanes subsequently developed. This is followed by the monoplane's ascendancy, the new ideas in aerodynamics here leading to significant drag reduction and increased speed. For this phase, data provided by the Royal Aircraft Establishment, which appear to be not widely known, are discussed in some detail, together with the Establishment's development of drag assessment methods. The survey then turns to the emerging jet age, ending with the early British swept-wing aircraft, forerunners of the Swift and Hunter. The influence of Reynolds number emerges in the survey but the transonic drag rise due to compressibility is not covered. It is hoped that this survey of aerodynamic drag reduction will be of interest to students new to the subject and also to those wishing to learn more of the development of aeronautical science.

1. Introduction

This paper is, in one sense, an appendix to two earlier papers published in this Journal. The first⁽¹⁾ described the evolution of our understanding of the aeroplane's lift and drag forces. This, in part, served as the basis of the author's Royal Aeronautical Society Cody Lecture in November 2015 given to the Society's Farnborough Branch. The second paper⁽²⁾ described the evolution of the Spitfire's aerodynamic design and sprang from the author's lecture on that subject given to the Society's Spitfire Seminar at Hamilton Place in September 2016. Both lectures included material not covered in the two papers, consisting of basic aerodynamic data for a variety of aircraft. Such data, particularly those amassed by the Royal Aircraft Establishment (RAE), Farnborough, around the period of the Second World War, might be of interest to a wider audience.

The Cody Lecture had the title 'Aerodynamics as the Basis of Aviation' and this provides the first part of this paper's title. To a modern audience this is clearly a no-brainer; a grasp of aerodynamics is nowadays accepted without question as an essential part of any successful aeroplane design and, indeed, has often been the lead technology. However, the lecture's title was taken from a lecture presented by Sebastian Finsterwalder (1862 – 1951) at Lausanne in 1909 and published⁽³⁾ in the following year. One suspects that Finsterwalder had adapted the title of an earlier book, widely read by aspiring aeronauts, written by the hang-gliding pioneer Otto Lilienthal (1848 – 1896). That book had the title *Bird Flight as the Basis of Aviation*⁽⁴⁾ and appeared in 1889. At that time and until the early years of the twentieth century, aerodynamics had been an entirely experimental activity in which various wing shapes were tested, shapes often loosely based on those in the natural world. Yet no one was able to say

why some wings performed better than others or indeed, more fundamentally, on what rational basis did any of them function. In contrast, Finsterwalder⁽³⁾ was suggesting that an emulation of bird flight no longer pointed the way forward; in future, guidance would be provided by this new science of aerodynamics. This, he believed, had at last acquired a rational basis resting on sound physical principles. In particular, he was drawing attention to the new circulation theory of lift developed by his Munich colleague, Martin Wilhelm Kutta (1867 - 1944), and the similar ideas of Frederick William Lanchester (1868 - 1946) in Britain. Indeed, on that basis the essential elements of modern wing theory emerged during the next decade, more details of which can be found in Reference 1.

Given the challenge implicit in Finsterwalder's lecture title, one is entitled to ask: how well did this new science do? That question provides the second part of this paper's title. In answer, the paper reviews certain core aircraft performance data over the years to illustrate the improvements brought about by the application of this new branch of the physical sciences. Two indicators of aerodynamic quality are surveyed, namely the drag coefficient at zero lift C_{D0} and the maximum lift-to-drag ratio $(L/D)_{max}$. The latter, however, is shown in Appendix 1 to be intimately related to C_{D0} and wing aspect ratio. A further important aerodynamic factor is the maximum lift coefficient C_{Lmax} , but this is not dealt with here. The main interest is in drag and what we might call the 'history of C_{D0} reduction'.

In this context the paper can also be seen as a supplement to Loftin's book *Quest for performance. The evolution of modern aircraft*⁽⁵⁾. Written by the former Chief Aeronautical Engineer at NASA's Langley Research Center, this provides a masterly survey of the technical development of the aeroplane which also emphasises the importance of the above two aerodynamic quantities. However, whilst Loftin⁽⁵⁾ draws his early examples from British and German aircraft of the First World War, later examples are predominantly those aircraft produced in the United States. Here, British examples drawn from the RAE's archive supplement Loftin's data. Moreover, in dealing with piston-engine aircraft, Loftin⁽⁵⁾ bases his calculations for C_{D0} entirely on engine power. But with the advent of ducted radiators and rearward ejecting exhausts in the mid-1930s, engine power became augmented slightly by the additional thrusts produced by these devices. Thus Loftin⁽⁵⁾ slightly underestimates the values of C_{D0} for the aircraft of what we might call the 'Spitfire generation'. Here thrust augmentation effects are included in the calculations leading to the data listed.

The next section of the paper describes the basic features of aerodynamic drag. There are two contributions, namely the drag induced by the trailing vortices of an aeroplane's lifting system and the drag due to the aeroplane's shape at its zero lift condition. The survey of basic aerodynamic data begins in Section 3 and deals with the period from the Wright Flyer of 1903 to the early 1930s, a period initially dominated by the biplane. Section 4 reviews the lecture given to this Society in 1929 by Bennett Melvill Jones. Entitled 'The Streamline Aeroplane', his lecture was, in essence, a plea for British designers to clean up their aerodynamic act. Aptly timed, it came within the short period during which designers were beginning to turn away from the well-understood biplane configuration of fabric-covered structural members, initially of wood, in favour of the greater efficiency offered by the monoplane of stressed-skin metal construction. Moreover, Jones was able, in effect, to

provide a target value for C_{D0} for his ‘Streamline Aeroplane’ to which designers might aim. Section 5 surveys the RAE’s aerodynamic data for the piston-engine monoplanes developed around the period of the Second World War. The final Section covers the beginning of the jet age. British units are used throughout, in keeping with the original aircraft performance data used.

2. Aerodynamic Drag and Its Evaluation

Before beginning this survey of aircraft drag reduction over the years, it is necessary to define drag, understand its origins and be specific as to the measure of it. In particular, we must be clear about the nature of those two aerodynamic quantities mentioned above, the drag at zero lift C_{D0} and $(L/D)_{\max}$.

Using his newly-established principles of dynamics, Isaac Newton (1643 – 1727) showed⁽⁶⁾ that the air resistance experienced by a body is proportional to the product of air density ρ , the square of the flow velocity V , and an area S which is characteristic of the body. Subsequently, a vast quantity of experimental evidence confirmed this fundamental proportionality. Thus the resistance component along an aeroplane’s direction of flight, the drag force D , is given by

$$D = \frac{1}{2} \rho V^2 S C_D. \quad (1)$$

The factor of $\frac{1}{2}$ was introduced in the late 1920s because the instrument used to obtain airspeed on aircraft and in wind tunnels, the Pitot-static tube, measures $\frac{1}{2}\rho V^2$ directly. As to the choice of the characteristic area S , the convention in aeronautics is that this is the total wing planform area. The quantity C_D , the ‘proportionality factor’ implicit in Newton’s relationship, is called the drag coefficient. Equation (1) shows that C_D is simply a number having no dimensions since both D and $\rho V^2 S$ have the dimension of force, lbs in the British system or newtons in Système International (SI) units. The value of this non-dimensional number is not a universal constant but, broadly speaking, depends on the shape of the aircraft and its attitude to the airstream. Thus it provides a measure of how drag-prone is the aircraft; for drag reduction, the lower its value the better.

To give some idea of the range of C_D values encountered, a flat plate held normal to an airstream has a C_D value a little over unity, the drag coefficient being based on its planform area S . This is also its frontal area, the area ‘seen’ by the approaching flow. A circular cylinder, for which S is taken to be the ‘seen’ frontal area, the product of diameter and span, has a C_D value only slightly less than this. A well-streamlined aerofoil, when reared up through 90° so as to present its under-surface head-on to the airstream in a very un-streamlined posture, also has a high C_D value, based on its planform area S , which is similar to those of the plate and the cylinder. In contrast, that aerofoil set at zero lift and small incidence has a C_D value which is roughly one hundredth of these values. Such an aerofoil has a maximum thickness of, say, one tenth of its chord. Thus its C_D value *based on its frontal area*, the product of maximum thickness and span, is ten times higher than that based on its planform area, yet ten times less than that of the cylinder. The practical significance of

these convoluted C_D examples, however, is revealed once they are translated into actual drag forces. It follows from the above that a wing having this aerofoil section set at low incidence and zero lift has the same drag at the same airspeed as a circular cylinder, or a wire, of the same span but of a diameter one tenth the maximum thickness of the aerofoil. This provides an indication of the scale of the drag experienced by the early biplanes and those few monoplanes of the early years of powered flight, festooned as they were with the struts and bracing wires needed for structural security.

As explained in Reference 1, the airflow close to a surface is slowed by friction, and the role of the thin, highly viscous boundary layer in this is crucial to the explanation of the drags described above. For the aerofoil at low incidence, it is its streamlined shape which controls the boundary layer's behaviour, persuading it to remain attached so as to separate only at the sharp trailing edge. Consequently the drag is created solely by the attached boundary layer, is relatively small and is mainly due to viscous skin friction. In contrast, the situation for the normal plate and the cylinder is quite different. In the case of the plate the boundary layer separates at its sharp edges; for the cylinder separation occurs near its maximum thickness. In both cases, separation results in wide wakes possessing low pressures, partial vacuums which suck the bodies backwards rather more than they are pushed rearwards by the flow's higher pressure impinging on their forward surfaces. It is this large pressure imbalance which is the dominant contributor to their high drags, not skin friction.

Little of this was understood until the early years of the twentieth century. The boat builders of antiquity must have been aware that streamlined shapes are advantageous but this does not appear to have prompted wider use of the idea. There were, however, moments of insight as the years progressed. The 'Father of Aeronautics', George Cayley (1773 – 1857), for example, produced a streamlined shape in 1809, based on his measurements of a trout⁽⁷⁾. He explained his thinking in the last of his triple papers⁽⁸⁾ published in 1810, pointing out that the shape of the rear of a body is as important as the front in reducing resistance. Without a tapered rear, he explained, "a partial vacuity" would be created, its suction thereby increasing the resistance. This, it must be added, went against current opinion, which held that it was the shape of the front of a body, not its rear, which determines resistance.

That all this might be in some way related to the air's viscosity seems not to have occurred to the nineteenth century's budding aeronautical community. Indeed, as late as 1891 Samuel Pierpont Langley (1834 – 1906), sometimes credited with coining the term 'aerodynamics', asserted⁽⁹⁾ that the value of the air's viscosity coefficient was far too small to be of any influence. An entirely contrary view emerged in the lecture delivered by Ludwig Prandtl (1875 – 1953) to the mathematical congress held at Heidelberg in 1904⁽¹⁰⁾. In this he pointed out that it was the conjunction of the air's extremely small viscosity coefficient and the enormous velocity changes within the thin boundary layer surrounding the surfaces of a body which creates significant skin friction drag. For what we now call laminar flow, in which the motion is smooth and devoid of random irregularities, he showed that for a flat plate at zero incidence the drag coefficient C_D is proportional to $Re^{-1/2}$. Here Re is the Reynolds number, a further dimensionless quantity which expresses the ratio between forces due to inertia and viscosity, and is given by

$$\text{Re} = \rho V \ell / \mu, \quad (2)$$

where ℓ is the plate length and μ the viscosity coefficient. Using the flow equations for the laminar boundary layer developed by Prandtl ⁽¹⁰⁾, his student Paul Richard Heinrich Blasius (1883 – 1970) obtained ⁽¹¹⁾

$$C_D = 2.654 \text{Re}^{-1/2}. \quad (3)$$

Experiment has confirmed this basic result although more accurate calculation gives the numerical coefficient as 2.656. At the extremely high Reynolds numbers experienced in flight, however, the laminar boundary layer is found to be unstable and trips into turbulence. For drag estimation with such boundary layers, reliance has had to be placed more on experimental evidence. As we shall see in Section 4, the C_D relation for turbulent flow over a flat plate takes a form similar to equation (3) although both the coefficient and the power to which Re must be raised are rather different.

Prandtl's lecture ⁽¹⁰⁾ of 1904 also explained the circumstance in which boundary-layer separation occurs. In passing around a body, the flow exterior to the boundary layer initially accelerates up to the body's maximum thickness but thereafter decelerates toward the rear. If this deceleration is too severe, the boundary-layer flow, already retarded by viscous action, may simply stop. Subsequently the boundary-layer flow peels away from the surface, exhibiting the phenomenon of boundary-layer separation which is the cause of the wide low pressure wake and excess drag. This, then, provides the reason for streamlining; the long tapered tail produces gentle deceleration so that separation is avoided. As to the effect of sharp edges such as those on the normal plate described above, the flow initially accelerates rapidly in attempting to round the edge but then promptly decelerates so severely that separation at the edge is inevitable. This also occurs at the sharp trailing edge of an aerofoil but, as Reference 1 explains, it is by this deliberate enforcement of boundary-layer separation there that this fundamental action of viscosity is used to generate the lifting system of a wing.

As to the lift L , the force component perpendicular to the flight direction, this mimics equation (1) by taking the form

$$L = \frac{1}{2} \rho V^2 S C_L. \quad (4)$$

Although we are mainly interested in the drag coefficient C_D , nonetheless the lift, and its non-dimensional coefficient C_L , enter the drag story. As explained in Reference 1, due to their wings' lift forces being generated continuously by the circulatory or bound vortices about them, all aeroplanes in flight inevitably create a system of trailing vortices in their wakes. These vortices produce a contribution to an aeroplane's drag called induced drag. By the close of the First World War the sound theoretical basis of this wing behaviour had emerged from Prandtl and his Göttingen associates ^(12, 13). Hermann Glauert of the RAE (Figure 1), who explained these ideas to a Britain largely innocent of such transformative advances, showed ⁽¹⁴⁾ that the induced drag coefficient C_{Di} is given by

$$C_{Di} = k C_L^2 / (\pi A). \quad (5)$$

Here A is the wing aspect ratio defined as the wing span divided by the average chord (the fore and aft dimension of the wing planform), or alternately as $(\text{wing span})^2 / (\text{wing planform area } S)$. The factor k has a minimum value of unity, which is obtained for a

monoplane wing alone experiencing an elliptic distribution of lift loading. The latter is most easily achieved by the use of an elliptic planform wing shape; other shapes produce k values slightly higher than unity. However, further contributions to k arise from the lifting systems of the complete aircraft, notably the tailplane and, in some cases, the fuselage itself. Thus arriving at a k value for a complete aircraft is often problematic and relies on wind-tunnel and flight-test data. As related in Reference 2, it is thought that Supermarine, for example, used the value $k = 1.15$ drawn from experience with the Spitfire. Biplanes and multiplanes produce further complexities in k 's estimation since the trailing vortices of the individual wings mutually interact in creating the total induced drag. Glauert⁽¹⁴⁾, for example, calculated that $k = 1.58$ for biplane wings of rectangular planform and equal spans, aspect ratio 6, and a gap-to-span ratio of 1/6. Here roughly 90% of the increase in k above unity comes from the biplane correction, the remaining slight correction being due to the fact that the rectangular wings' planforms do not produce ideal elliptic loading.



Figure 1. Hermann Glauert FRS (1892-1934)*
Source: Royal Aeronautical Society
(National Aerospace Library)

The coefficient for the total drag experienced by an aeroplane, C_D , is then

$$C_D = C_{D0} + C_{Di}. \quad (6)$$

Here C_{D0} is the drag coefficient at the zero lift condition, the coefficient representing the drag caused by the airflow behaviour around the aircraft at this condition for which, there being no trailing vortices, the induced drag is also zero. The value of C_{D0} partly depends on the effects

* Born in Yorkshire, Hermann Glauert won a mathematics scholarship to Trinity College Cambridge and in 1916 joined the Aerodynamics Department of the Royal Aircraft Factory, Farnborough (from 1918 the RAE). His visit to Göttingen after the close of the First World War provided him with the work there on boundary layers and wing theory. In his subsequent career he introduced improved mathematical methods to wing theory, extending this to a wide variety of aerodynamic problems. He became Head of the Aerodynamics Department in 1931 but was killed in a tragic accident in 1934. He was the first of a number of RAE staff to become Fellows of the Royal Society.

of the boundary layer such as surface skin friction and, if present, boundary-layer separation, but also includes drag contributions caused by excrescences. The boundary-layer drag contribution is often referred to as profile drag whereas that due to excrescences and such is called parasite drag. Unlike induced drag, or C_{Di} , which can be predicted with reasonable accuracy, as above, the prediction of C_{D0} is more problematic, as we shall see as the drag story unfolds.

An estimate of C_{D0} can be obtained from wind-tunnel tests, simply by measuring the aircraft model's drag at zero lift. However, because the model is smaller than the full-scale aircraft and the testing speed usually much lower than that achieved in full-scale flight, the problem of the 'scale' or Reynolds number effect (see, for example, References 1 and 2), can result in inaccurate values for the full-scale value of C_{D0} . Values of higher accuracy are obtained by flight testing at full scale. In this case knowledge of the engine power or thrust required to achieve the measured airspeed at a given altitude is used to calculate C_D . Also from the airspeed and the additional knowledge of the aeroplane's weight the value of C_L at this flight-test condition can be obtained from equation (4). Equation (5) then provides an estimate for C_{Di} so that, from equation (6), the value of C_{D0} is obtained. More details of this calculation procedure are given in Appendix 2.

At this stage it is useful to see how C_L , C_D , and $C_L/C_D (= L/D)$ for an aeroplane vary throughout the useful incidence range. Figure 2 illustrates these variations, although the graphs are not drawn to a common vertical scale but merely illustrate the trends. Thus C_L increases almost linearly with incidence until the graph curls over to a maximum. At this point wing stall occurs around C_{Lmax} , the stall being caused by gross boundary-layer separation due to the wing upper surface's flow deceleration becoming too severe.

It is important to understand that, at whatever point an aeroplane reaches in its flight envelope, the aeroplane must be at some point on the $C_L \sim$ incidence graph. For example, at high speed the lift L is 'generated' mainly by the $\frac{1}{2}\rho V^2$ term in equation (4) and the aeroplane flies at a low value of C_L /low incidence. Conversely, at low speed a high C_L /high incidence is required.

According to equation (5), C_{Di} varies as C_L^2 so the C_D graph shows a quadratic curve rapidly rising upward from its initial C_{D0} value as incidence increases. For drag analysis, flight-test results are often obtained at the higher end of the speed spectrum so that, as mentioned earlier, C_L is low, typically around 0.1. In this case C_{Di} is small, usually around 5% of C_D .

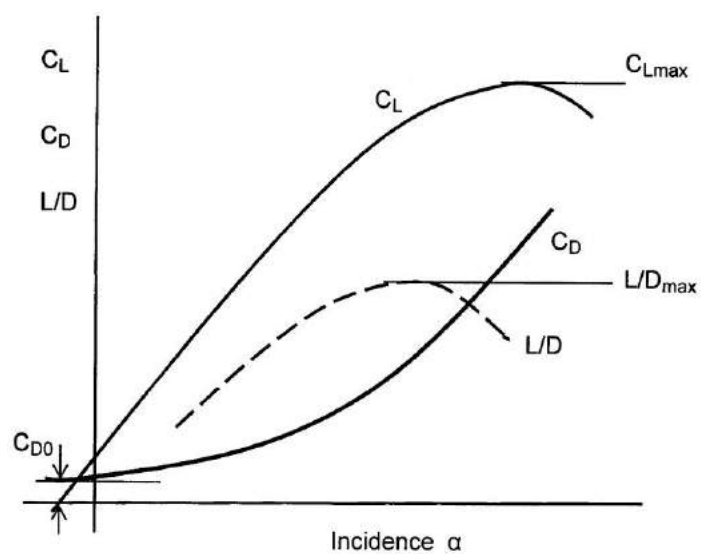


Figure 2 Variations of C_L , C_D and L/D with wing incidence α

Consequently, for the calculation of C_{D0} from flight-test data, an accurate value for k in the estimation of C_{Di} is not essential. Indeed, in Section 5 it will be found that, in British practice during the 1940s, for simplicity the value of k selected was unity, the value for a wing alone experiencing the ideal elliptic loading situation.

Because C_{Di} varies as C_L^2 the graph for L/D shows a maximum value, not at C_{Lmax} but at some intermediate C_L value. In Appendix 1 it is shown that a high value of $(L/D)_{max}$ produces the beneficial effects of small gliding angles and, for powered flight, enhanced range. The ratio is thus an indicator of aerodynamic efficiency and it is therefore useful to predict its value. The analysis for this is included in Appendix 1, the result being that

$$(L/D)_{max} = \frac{1}{2}(\pi A / (k C_{D0}))^{1/2}. \quad (7)$$

Clearly, in order to produce a high value of $(L/D)_{max}$ it is necessary to have C_{D0} as small as possible whilst the aspect ratio A should be as large as structural limits and mission requirements allow. Because of the form of equation (7), the estimation of $(L/D)_{max}$ from that equation requires a reasonably accurate value of k to be selected, unlike the case above in the estimation of C_{D0} .

Appendix 1 also includes a discussion of Figure 2's other features, particularly those related to the early wing theories proposed by Prandtl and his Göttingen colleagues and by Lanchester in Britain.

During the first forty or so years of powered flight, propulsion was provided almost exclusively by piston-engine/propeller combinations. The engine powers required for this phase of development are discussed in Appendix 2, in which it is shown that engine power is related to the cube of aircraft speed. As an illustration of what might be called the 'tyranny of V^3 ', it is shown that an aeroplane with the high drag characteristics and wing area of the Wright Flyer would have required an engine power of about 10,000 hp to achieve a maximum speed of around 300 mph. That such a speed was achieved with powers around a tenth of that value is a tribute not only to engine designers but also to the successful application of the new ideas in aerodynamics. The latter are shown in Appendix 2 to have reduced the drag of the Flyer by a factor of ten. The achievement is all the more remarkable in that it was accomplished in little over thirty years after the Flyer. That said, the basic guidelines for this advance – the boundary-layer and wing theories - were in place ten years earlier or, to re-iterate an earlier point, a decade after Finsterwalder's lecture.

Appendix 2 also includes the effects of thrust augmentation made possible by the introduction of ducted radiators and rearward-ejecting exhausts. In addition, the analysis underlying the British practice in drag assessment is explained, in which all drag contributions measured either in wind tunnels or in flight tests are scaled down to drag data at a speed of 100 ft/s at sea level. This made it easier to compare the drag characteristics of one aircraft type with another.

3. From the Wright Flyer to Aircraft of the Early 1930s

It would be appropriate to begin this survey of aircraft drag data with those for the first aeroplane to achieve powered, controllable flight, the Wright Flyer flown at Kitty Hawk in December 1903. However, little can be deduced from the short flights achieved. Luckily, as part of the centenary celebrations of the Wrights' achievements, wind tunnel results for a scale model of its development, the Flyer 3 of 1905, are now available. Although the main interest of the paper by Padfield and Lawrence⁽¹⁵⁾ centres on the Flyer 3's unusual flight dynamics, its basic aerodynamic data were obtained from wind-tunnel tests of a one-eighth scale model. These data are given in Lawrence's doctoral thesis⁽¹⁶⁾ and it is felt that data for the 1903 Flyer would not differ significantly from these. Lawrence⁽¹⁶⁾ obtains $C_{D0} = 0.1$ whereas $(L/D)_{\max}$ is around 5.6 and these results head Table 1 below. Using Glauert's value of $k = 1.58$ for an equal span biplane, wings of aspect ratio 6 and gap-to-span ratio $1/6 (= 0.167)$ [the Flyer 3's aspect ratio is 6.47 and gap-to-span ratio 0.15], equation (7) yields $(L/D)_{\max} = 5.7$, a result close to that given by Lawrence⁽¹⁶⁾. Table 1's other data are taken from Loftin⁽⁵⁾, to which have been added the year of first flight.

Table 1's data cover the initial, largely biplane phase of aeroplane development followed by the early years of the aerodynamically cleaner monoplane. In the former category, the examples include a few monoplanes, also often heavily braced, but all possessing such additional drag-producing features as open cockpits and fixed undercarriages.

Table 1 Zero lift drag, aspect ratio and maximum lift/drag, aircraft 1903 to 1935

	C_{D0}	Aspect ratio A	Lift/drag $(L/D)_{\max}$
Wright Flyer 3 (1905)	0.10	6.28	5.6
B. E. 2c (1914)	0.037	4.47	8.2
Fokker E III (1915)	0.077	5.70	6.4
Airco DH-2 (1915)	0.043	3.88	7.0
Airco DH-4 (1916)	0.042	4.97	8.1
Albatros D-III (1916)	0.047	4.65	7.5
Sopwith F.1 Camel (1916)	0.038	4.11	7.7
Fokker Dr. 1 Triplane (1917)	0.032	4.04	8.0
Junkers D-I (1917)	0.061	5.46	7.0
Fokker D-VIII (1918)	0.055	6.58	8.1
Handley Page 0/400 (1918)	0.043	7.31	9.7
Fokker F-2 (1920)	0.047	7.10	9.4
Handley Page W8f (1924)	0.055	4.67	7.1
Ford 5-AT (1926)	0.047	7.26	9.5
Ryan NYP (1927)	0.038	6.63	10.1
Northrop Alpha (1930)	0.027	5.93	11.3
Lockheed Vega 5C (1931)	0.028	7.65	11.4
Lockheed Orion 9D (1931)	0.021	7.01	14.1
Boeing 247D (1933)	0.021	6.55	13.5
Douglas DC-3 (1935)	0.025	9.14	14.7

The Royal Aircraft Factory's B. E. 2c is a particularly interesting case since it emerged so early and, in terms of C_{D0} and $(L/D)_{max}$, it appears to perform well. Yet as Loftin⁽⁵⁾ points out, it was underpowered with a slow top speed and a poor rate of climb. One virtue appeared to be its high stability, yet this resulted in sluggish manoeuvrability in defence which earned for it the term 'cold meat' from German fighter pilots. Readers are encouraged to study the well-judged assessments Loftin⁽⁵⁾ provides for many of these First World War aircraft, particularly his reasons for why the few monoplanes (Fokker E III, Junkers D-1, Fokker D-VIII) did little better than their biplane contemporaries. Suffice it to say that many factors determined the usefulness or otherwise of aeroplanes deployed in that conflict, and low drag was probably not the foremost consideration.

Economic considerations in commercial aviation became more of a driving force for aerodynamic improvement during the late 1920s, particularly in the United States. Further impetus for drag reduction arose when national prestige was at stake; one way or another, money could be found to support such endeavours as the Schneider Trophy contests and the MacRobertson Air Race from London to Melbourne in 1934.

A significant decrease in C_{D0} can be detected in Table 1 with the advent of the more streamlined monoplane, examples being the Northrop Alpha and the two Lockheed aircraft, the Orion being notable for its retractable undercarriage. Here the monoplane also began to benefit from the adoption of solid-skin construction, the skin now assisting in carrying the main structural loads. Table 1's last two types, the Boeing and Douglas aircraft, provide examples in which the further step of all-metal construction had been taken. Together with this and the adoption of retractable undercarriages came the use of enclosed cockpits and means to reduce engine drag: cowlings for radial engines and ducted radiators for liquid-cooled engines. Further aerodynamic refinements such as wing-root fillets and better surface finishes produced yet more drag improvements. The resulting reductions in C_{D0} , together with the use of higher wing aspect ratios for commercial aircraft, resulted in improvements in $(L/D)_{max}$, as Table 1 shows.

Anderson⁽¹⁷⁾ uses such data to illustrate these phases of development by constructing a diagram showing a series of three downward steps in C_{D0} values as the years progressed. In this diagram the first, largely biplane phase (1910 – 1925) has an average C_{D0} value around 0.045, but with notable scatter as Table 1's data indicate. For the second phase (1927 – 1947) in which the piston-engine monoplane takes the stage, the average C_{D0} value drops to about 0.027, but again with significant scatter. More data for this phase, drawn from the large RAE archive, are given in Section 5 below. According to Anderson⁽¹⁷⁾ the final phase, that of the jet-propelled aeroplane, produced an average C_{D0} of 0.015 and British data for the early years of this phase are given in Section 6.

4. B. M. Jones and the 'Streamline Aeroplane' (1929)

The importance of the lecture⁽¹⁸⁾ given by Jones (Figure 3) to the Royal Aeronautical Society in 1929 has been mentioned in Section 1. At this stage of his notable career, by now a

leading member of Britain's Aeronautical Research Committee (ARC), he was well-placed to press for aerodynamic improvements in British aircraft.

Jones began his lecture⁽¹⁸⁾ by reminding his audience of "the effortless flight of the sea birds and the correlated phenomenon of the beauty and grace of their forms. We all possess a more or less clear ideal of what an aeroplane should look like; a kind of albatross..." He went on to complain that "progress towards this ideal, so far as the general purpose craft is concerned is, we must admit, painfully slow. It has seemed to me that a contributory factor to the slowness of this evolution has been the lack of any generally understood and easily visualised estimate of what could be achieved were the difficulties in the way of realising the ideal form overcome. There is a natural tendency to decide on one day that the gain – say 20 per cent. on the total drag, or 7 per cent. on the speed – to be had by spending endless trouble on improving the undercarriage design, is not worth the trouble; on the next day to come to a similar conclusion about the drag of the engine cooling apparatus; on the next day about the wires, struts and minor excrescences; and on the next about the pilot's view; omitting to notice that if all the improvements were made at once the total gain would not be some insignificant percentage of the whole, but might reduce power consumption to a small fraction of its original value and so extend the range and usefulness of the aeroplane into realms which would otherwise be unattainable."

Jones⁽¹⁸⁾ then explained that there are two distinct types of drag, as outlined in Section 2, namely induced drag and the drag due to the aeroplane's shape. The former, he pointed out, can be calculated with reasonable precision using, in effect, equation (5) above. He demonstrated that, at the high end of the speed spectrum, this induced drag is small, typically 5% of the total. Thus it is with the residual drag contribution that the main problem lies. He then proposed an aeroplane shaped so that excrescences and such are entirely absent, a shape so streamlined, so aerodynamically clean as to be devoid of parasite drag, that the only remaining drag contribution is that which cannot be eradicated, namely the profile drag due to the boundary layer. He rightly took the view that at the high Reynolds numbers of full-scale flight the boundary layer would largely be turbulent. To this should be added the point that all parts of an aircraft's surface infected by a propeller's turbulent wash will inevitably

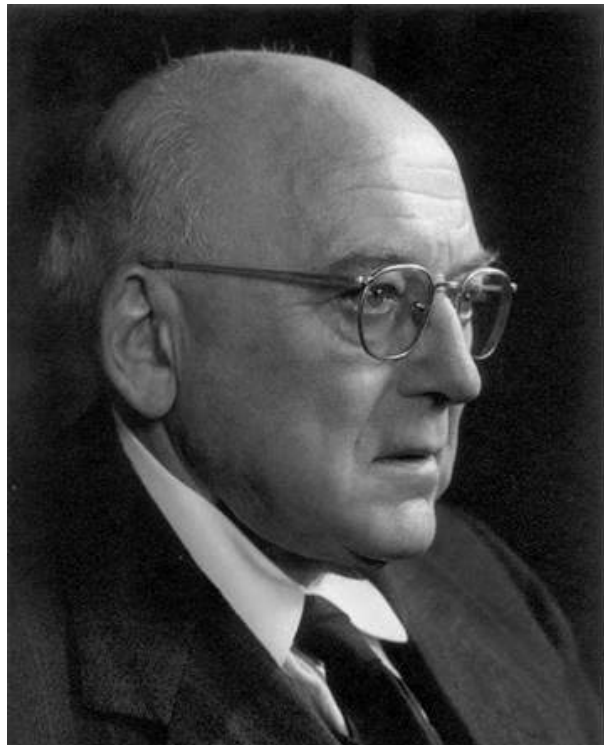


Figure 3 Bennett Melvill Jones FRS (1887 – 1975). He joined the Aerodynamics Department of the National Physical Laboratory in 1911, moved to the Royal Aircraft Factory in 1914 and in 1916 to the Air Armament Experimental Station, Orford Ness. A Cambridge graduate, he returned there in 1919 to become Francis Mond Professor of Aeronautical Engineering until retirement in 1952.

Image: Aircrew Remembered.
<http://aircrewremembered.com/>

be turbulent. For such conditions he replaced equation (3) for laminar flow with one based on experiment provided by Prandtl⁽¹⁹⁾ which, in the notation used here, is

$$C_D = 0.076 Re^{-0.15}. \tag{8}$$

With this relation for turbulent skin friction on flat plates, he produced, in effect, an estimate for C_{D0} for his ideal ‘streamline aeroplane’. The details of his calculations are given in Appendix 3, where it is seen that his target value, though not stated in such terms, is

$$C_{D0} = 0.0128. \tag{9}$$

Here bold italics are used to indicate that this C_{D0} value is for the clean aeroplane, a notation which will be used later in Section 5.

On the above basis, in effect, and by the use of equation (5) for C_{Di} , Jones⁽¹⁸⁾ constructed the fairly narrow band of theoretical curves shown toward the base of Figure 4. The horizontal ordinate here is the aircraft speed in miles per hour. Probably because he wished to present his data in a form which would appeal to his audience at that time, he chose as his vertical ordinate the quantity ‘Brake Horsepower per 1000 lbs weight’. Consequently, his theoretical curves had to be calculated for a range of wing loadings (weight/S) and also span loadings (weight/(span)²). Included in the figure are the data points for current aircraft, many of which are British biplanes, and these provide a truly graphic illustration of how far in excess of Jones’s ideal these were. The nearest to his theoretical curves is the monoplane Ryan NYP ‘Spirit of St. Louis’ (see Table 1) in which Charles Lindbergh had flown the Atlantic in 1927.

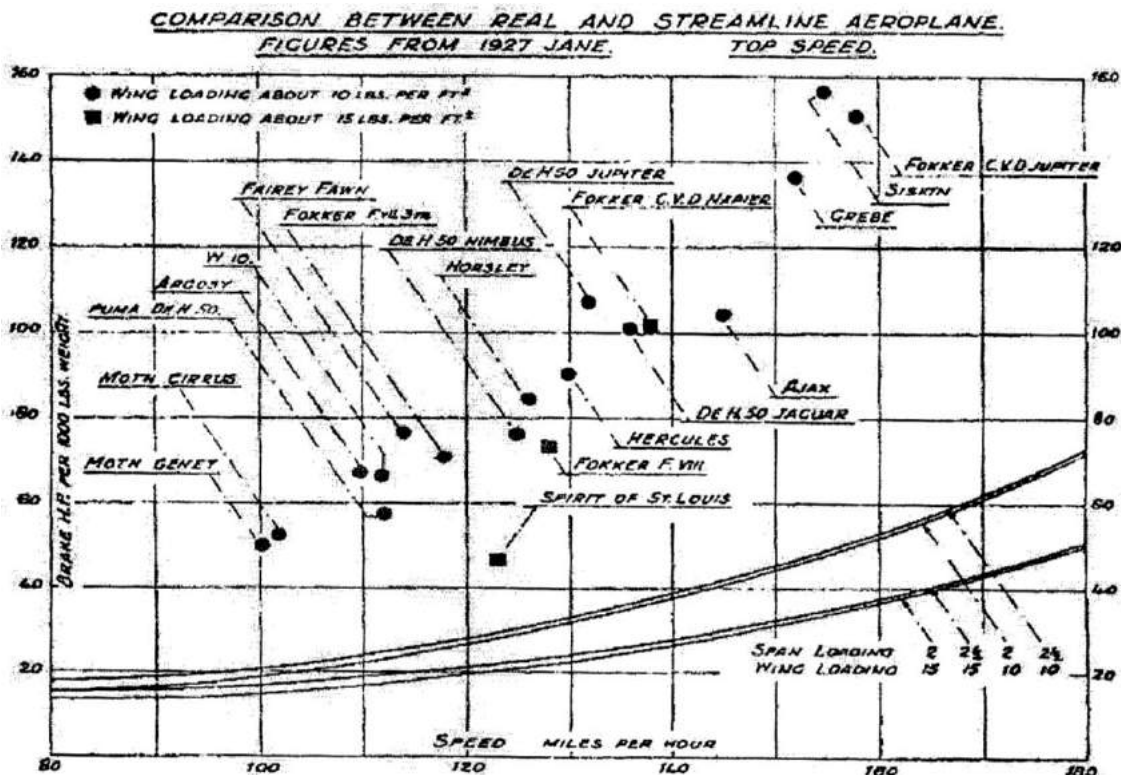


Figure 4 Power versus Speed; Jones, Reference 18

As was often the case during this period, the discussion following Jones's lecture, carefully recorded in its publication⁽¹⁸⁾, was almost as interesting as the lecture itself. The audience's response was somewhat mixed; whilst some clearly got the message, others were rather dubious. Charles Clement Walker (1877 – 1968) of de Havilland Aircraft, for example, reported that “an ordinary commercial aeroplane did attain from 60 to 67 per cent of the streamline speed”. He went on to list a number of excrescences and such which were, he felt, unavoidable on aircraft: “the undercarriage, all the bracing, the cooling of the engine, the cockpit”. He added that “in the case of commercial aircraft, which must have all sorts of other excrescences, it was difficult to foresee how far one could go towards eliminating the resistance. Such a machine had a radial engine sometimes at the front of the body, the cabin had to be ventilated by means of structures like ships' ventilators, sometimes there was a starting engine mounted outside the fuselage, and it did not matter very much what one did in the way of fairing after that. It would be interesting to know what Professor Jones thought about the amount that could be saved”. The transcript of the discussion records audience laughter at this point. The latter perhaps suggests that Walker's contribution was seen by some as apt criticism. Yet within the next few years a number of his listed drag creators were either eliminated or reduced in their effect. One such item was raised by George Herbert Dowty (1901 – 1975) who, whilst recognising the undercarriage as a significant drag creator, took the view that “the retractable undercarriage is not desirable because of the complicated retracting mechanism and the extra weight involved”. He went on to report that he was working on a fixed undercarriage of reduced drag. Though not germane to the current topic of drag reduction, it is worth noting that around this time similar reservations on the grounds of complexity and weight were expressed in the discussion following a lecture to this Society on variable pitch propellers⁽²⁰⁾.

In his response to Walker, Jones⁽¹⁸⁾ remarked that “Since power varies approximately as V^3 , the realised speed of 70 per cent of the streamline speed corresponds to an expenditure of power of about three times the streamline power for a given speed”. To Dowty he merely replied that he was “interested to hear of his efforts to tackle the problem”. As to matters raised by other audience members, much of their discussion turned into a debate on transition to turbulence, providing an interesting snap shot of the limited state of aerodynamic knowledge on this topic in Britain at that time. At one point David Randall Pye (1886 – 1960) asked if data for aircraft competing for the Schneider Trophy could be added to Figure 4. To this Jones replied that he had not included these aircraft since they were not comparable with the other aeroplanes in his figure. He added that “it would be interesting to see them worked out accurately by someone at the Air Ministry who has the facts at his fingers' ends”. Such data as are available to this author for the Supermarine S4 to S6B, together with the Spitfire's forerunner, the Type 224, are listed in Appendix 4. These are used to provide rather tentative values for C_{D0} .

At this point it is interesting to ask: was Jones's ideal, put here as $C_{D0} = 0.0128$, achieved in the subsequent drive to produce aerodynamically cleaner aeroplanes? The answer for the piston-engine era is that it was not. Taking the case of the Spitfire, one of the cleaner British military aircraft, we will find a C_{D0} value of 0.020 in the survey of Section 5 below. There it will be seen that its boundary-layer drag is about 58% of the total, indicating that if all other parasite drag contributions had been eradicated its C_{D0} value would have been 0.012, close to

Jones's ideal. But as we shall see, for practical reasons total parasite drag eradication was not possible. For the jet aeroplane era the results turn out to be rather better, as will become clear in Section 6.

Finally, to return to Jones's opening comments lauding the aerodynamic virtues of the albatross, we might ask: how well does that bird do? In 2005 Sachs⁽²¹⁾ reviewed the various estimates of albatross performance made between 1932 and 1982. Estimates for C_{D0} ranged between 0.020 and 0.048 and, for his calculations, he selected 0.033. Aspect ratio estimates varied between 15 and 20 so that $(L/D)_{\max}$ values ranged from 18 to 24.6. For the latter ratio, Sachs⁽²¹⁾ selected a value of 20. It appears then that with regard to C_{D0} the piston-engine fighters of the Spitfire generation did really rather well in comparison.

5. Piston-Engine Monoplanes (1930s and 1940s)

5.1 Royal Aircraft Establishment figures of merit

With the arrival of the new generation of largely monoplane military aircraft in the mid-1930s, the RAE's Aerodynamic Staff felt the need to set down simple figures of merit when assessing aeroplane performance⁽²²⁾. The emphasis was on what they termed residual drag, the drag remaining once induced drag has been deducted. Residual drag, it will be recalled, has two contributions, the profile drag created by the boundary layer's action, and the parasite drag created by protrusions, excrescences, leaks from access panels and bomb doors and, in general, anything which creates departures from a well-streamlined clean form. The Aerodynamic Staff's report⁽²²⁾ issued in January 1937 introduced four figures of merit, two of which turned out to be C_{D0} and $(L/D)_{\max}$, the latter being seen as an indicator of transport efficiency (see Appendix 1). However, a third figure of merit appeared, this being the cleanness efficiency, a term which rapidly became renamed cleanness ratio, CR. This is another measure of the residual drag, and was defined as the ratio of the residual drag of the clean aeroplane, in other words the profile drag entirely due to the boundary layer, to the actual residual drag. As Jones⁽¹⁸⁾ had done (see Appendix 3), the profile drag due to the boundary layer was estimated using experimentally obtained flat plate skin friction formulae assuming a turbulent boundary layer throughout. In the notation adopted in Section 4, it follows that

$$CR = C_{D0} / C_{D0}. \quad (10)$$

Here, however, it must be understood that C_{D0} , the drag coefficient entirely due to the boundary layer on the clean aircraft, does not have the value assigned to it by Jones⁽¹⁸⁾, the result given by equation (9). That value was an average for the current aircraft surveyed by Jones in 1929. Now the evaluation of C_{D0} is tailored to each individual aircraft. Using the value for the skin friction coefficient appropriate to the flight Reynolds number as described in Appendix 3, that coefficient is then applied to the estimated total wetted area of that aircraft and finally C_{D0} is calculated knowing the ratio of the total wetted area to the wing planform area S .

The final figure of merit introduced in Reference 22 compared the residual drag of an equivalent flying wing, there being no other lifting surfaces, and the residual drag of the actual aeroplane. However, this criterion was dropped in the next report on the matter issued in October 1937⁽²³⁾.

Whilst the first report⁽²²⁾ provided performance data for fifteen recent aircraft, the second⁽²³⁾ added data for a further six: Hawker Hurricane, Supermarine Spitfire, Fairey Battle, Bristol Blenheim, Armstrong Whitworth Whitley and Handley Page Harrow. Of the first report's aircraft, the Avro 652 became the Anson. The less-well-known Burnelli UB-14A was an American lifting-fuselage airliner, the Hendy Heck built by Parnall Aircraft a four-seat cabin monoplane, the Martin B-10 the U S Army Air Corps' first all-metal monoplane bomber, the Caudron 460 a French racing monoplane and the Miles M.6 Hawcon was a research monoplane built for the RAE on which four wing thicknesses could be investigated.

The aircraft included in the two reports^(22, 23) are brought together in Table 2 which lists their data of more immediate interest here such as C_{D0} and $(L/D)_{max}$. Also included are cleanliness ratio (CR) and propeller efficiency η , the latter being listed because those of its values above 0.80 seem rather high when compared with later evaluations. As to cleanliness ratio, the Heinkel, Caudron, Comet and Falcon lead the field with the Spitfire the best of the newer six military aircraft. The Heinkel He. 70 with its extraordinarily low value of C_{D0} is the Kestrel engine version bought by Rolls-Royce. Since this loomed large in RAE thinking at this time, the subsequent extensive investigations into its performance are discussed separately in Appendix 5. As will emerge presently, the Hurricane listed in Table 2 is the prototype. It is likely that the Spitfire listed is also the prototype since its engine is stated to be the Rolls-Royce PV 12.

5.2 Drag measurement by flight testing

Flight testing of the British aircraft was conducted either at the RAE or the Aeroplane and Armament Experimental Establishment (A&AEE), Martlesham Heath near Ipswich, or, in the case of the two flying boats, the Marine Aircraft Experimental Establishment, Felixstowe. Except for the Heinkel assessed by Rolls-Royce, data for foreign aircraft were obtained from reliable foreign sources.

As equation (7) indicates, aircraft having low values of C_{D0} and moderate to high aspect ratios benefit in terms of $(L/D)_{max}$. However, the latter's values listed in Table 2 are probably a little high. In evaluating k the wing alone was considered, taking account of planform shape, taper ratio and the biplane factor as appropriate. Thus for the complete aircraft it is likely that k would be slightly higher and this, by equation (7), would reduce slightly the values of $(L/D)_{max}$.

As indicated in Table 2, the second report⁽²³⁾ states that the engine powers for the Hurricane, Spitfire and Battle are suspected as being rather high. This, in conjunction with the perhaps too high values of η , suggests that the propeller thrusts for these three aircraft are too high, in

which case one would expect C_{D0} to be rather lower. On the other hand, as yet the thrust effects of ducted radiators have not been included in the assessments, effects which would raise C_{D0} values. Perhaps in these cases the engine power over-estimation and the augmentation effects have, by chance, cancelled each other out since the later, more accurate C_{D0} values for the Hurricane and Spitfire are essentially those given in Table 2.

Table 2 Figures of merit from flight test measurements

	Propeller efficiency η	Zero lift drag C_{D0}	Cleanness ratio CR	$(L/D)_{max}$
Airspeed Courier (1933)	0.755	0.0256	0.390	15.5
Avro 652 (Cheetah V) (1935)	0.755	0.0266	0.413	14.4
Avro 652 (Cheetah VI) (1935)	0.78	0.0262	0.424	14.5
Burnelli UB 14A (1934)	0.74	0.0252	0.297	14.9
DH 88 Comet (1934)	0.83	0.0197	0.531	19.0
Gloster Gauntlet (1933)	0.82	0.0314	0.329	10.0
Gloster Gladiator (1934)	0.825	0.0260	0.349	10.5
Heinkel He 70 (1932)	0.82	0.0150	0.540	18.5
Hendy Heck (1934)	0.765	0.0260	0.394	13.5
Martin B. 10 (1932)	0.77	0.0286	0.321	14.3
Caudron 460 (1934)	0.850	0.0215	0.564	15.3
Miles Falcon (1934)	0.79	0.0228	0.520	15.6
Miles M.6 Hawcon (1935)	0.80	0.0240	0.435	14.5
Short R 24/31 (1933)	0.72	0.0540	0.212	10.1
Short Singapore II (1930)	0.76	0.0514	0.341	8.61
Hawker Hurricane (1935)*	0.855	0.025	0.350	14.0
Supermarine Spitfire (1936)*	0.855	0.020	0.430	15.0
Fairey Battle (1936)*	0.79	0.023	0.380	14.5
Bristol Blenheim (1935)	0.825	0.026	0.350	14.0
Arm. Whit. Whitley (1936)	0.810	0.025	0.360	13.0
Handley Page Harrow (1936)	0.810	0.032	0.350	13.0

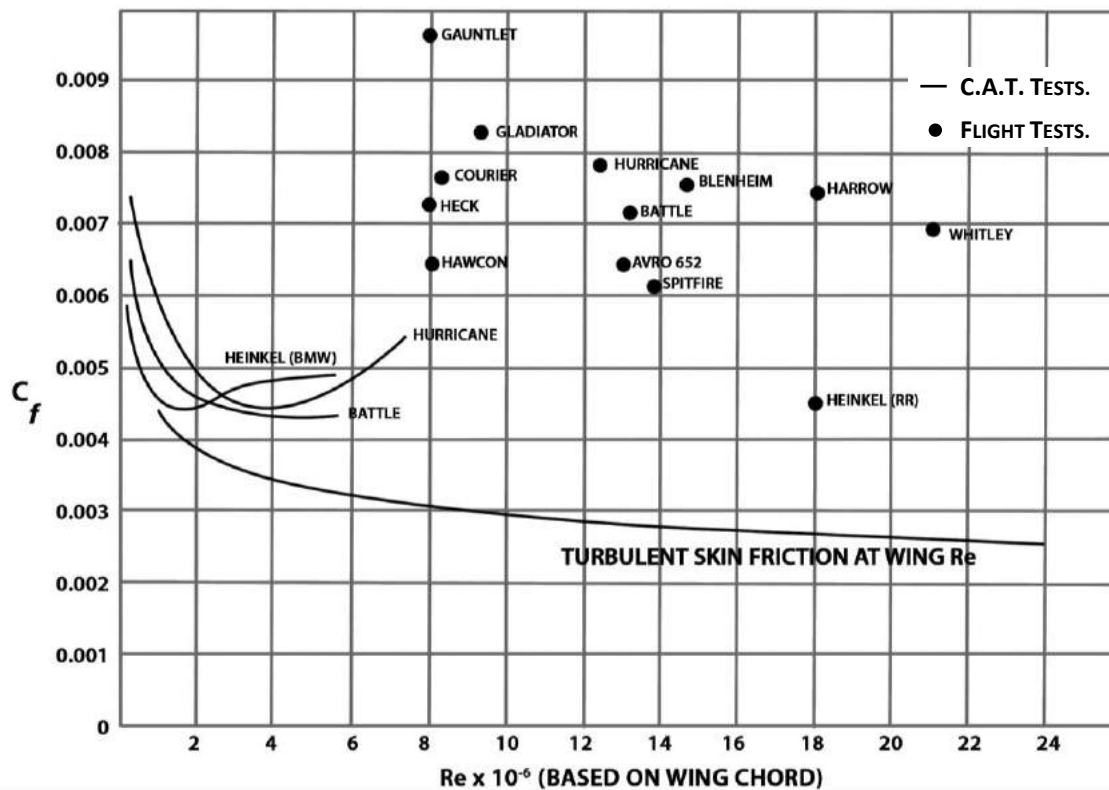
* Engine Power Estimates may be 5 – 10% too high

Source: RAE Staff, References 22, 23

5.3 Flight test and wind tunnel comparisons

The second report⁽²³⁾ includes a graph (Figure 5) showing a comparison of data obtained from flight tests and the Compressed Air Tunnel (CAT) at the National Physical Laboratory (NPL). The CAT was capable of reaching significantly higher Reynolds number (Re) values than more conventional wind tunnels. In Figure 5 the horizontal ordinate is Re based on

wing chord, whereas the vertical ordinate is the coefficient C_f . C_f is the drag coefficient at zero lift, C_{D0} , but based on the aircraft's wetted area rather than its wing planform area S . In Jones's notation⁽¹⁸⁾ (see Appendix 3), E being the wetted area, $C_f = S C_{D0} / E$. Figure 5's lowest continuous curve is the result for turbulent boundary layers on flat plates similar to



COMPARISON OF C.A.T. AND FLIGHT DRAG MEASUREMENTS

Figure 5 Modified drag coefficient C_f against Re . Source, Reference 23

that used by Jones⁽¹⁸⁾. The other curves are the CAT results for models of the Hurricane, Battle and the BMW-powered version of the Heinkel He. 70. The data points for the aircraft indicated are obtained from flight tests. These are at significantly higher Re values than those achievable even in the CAT and the figure thus illustrates the difficulty in drag prediction at full scale using wind-tunnel data. The wind-tunnel curve for the Heinkel might extrapolate quite well to the data point for the full-scale aircraft, but the same cannot be said for the Hurricane and Battle curves. As described in Section 3 of Reference 2, it was this difficulty which Collar⁽²⁴⁾ addressed in 1940 in his performance comparison of the Hurricane and the Spitfire. His essential point was that it is crucial to compare like with like when relating CAT data with full-scale results. Once various items of parasite drag had been deleted from his drag assessments of the full-scale aircraft, so that the model and full-scale aircraft were similar, the CAT results extrapolated quite well to the full-scale results.

To return to the cleanliness ratio, CR, it is interesting to use its values together with those for C_{D0} in Table 2 to obtain estimates for C_{D0} . Using equation (10) and taking the cases of the best of the monoplanes and biplanes, the Heinkel and the Gladiator respectively, the following results are obtained:

Heinkel He. 70 $C_{D0} = 0.008$

Gladiator $C_{D0} = 0.009$.

As indicated in Appendix 3, these are close to the value Jones⁽¹⁸⁾ would have obtained ($C_{D0} = 0.0086$) had he not allowed a significant increase to boost his flat plate turbulent boundary-layer drag calculations. The above two results suggest that the RAE Aerodynamic Staff were allowing no such increases but were sticking rigorously to the turbulent boundary-layer curve of Figure 5 in their estimation of boundary-layer drag. Three points are worth raising here. Firstly, how accurate was this turbulent boundary-layer drag assessment method based on flat plate data? The answer, shortly to be given, was that it underestimated this drag contribution. Secondly, as Figure 5 illustrates, C_{D0} estimation based on maximum power and speed data provides a snap-shot value at only one Re value. But from take-off to maximum speed an aircraft's speed can increase by a factor of five or six; the aircraft thus traverses a corresponding range of Re values over which the boundary-layer drag contribution to C_{D0} will vary. Thus some variation in C_{D0} , albeit slight, will occur over an aircraft's speed range due to this Re effect. Finally, despite possible inaccuracies in boundary-layer drag estimation, the CR values for many of the aircraft listed in Table 2 are very low. Thus it was perceived that there was a major problem with regard to parasite drag and its prediction.

5.4 Sources of parasitic drag

In August 1938 Morgan (Figure 6) used the assessments provided by the two RAE reports^(22, 23) in an attempt to pin down the sources of parasite drag⁽²⁵⁾. For this he estimated the drag contributions from various aircraft parts for five sample aircraft. Four of these, the Handley Page Harrow, Armstrong Whitworth Whitley, Gloster Gladiator and the Hawker Hurricane, have similar CR values, while the fifth, the Heinkel He. 70 with its larger CR value chosen for comparison, served as his yardstick for cleanness. This exercise was prompted, as Morgan⁽²⁵⁾ puts it, "to find, if possible, the reason for the unexpectedly low cleanness efficiency of the Hurricane prototype", thus confirming that it is this aircraft which appears in Table 2. The total drag in each case is the residual drag which remains after the induced drag has been deducted. His results are listed in Table 3, his drag categories, he admits, being rather arbitrarily chosen.

Morgan⁽²⁵⁾ drew on 45 data sources (31 RAE and ARC reports, 12 NACA reports and 2 others) to estimate the various drag subtotal contributions listed in the first part of Table 3. In additional data tables not reproduced here, he provided more detailed drag estimates for



Figure 6 Morien Bedford Morgan FRS (1912 – 1978).

Source: Royal Aeronautical Society (National Aerospace Library)

individual items contributing to these subtotals. The more detailed individual drag data for the Hurricane will be used later so as to compare his results with those of Collar⁽²⁴⁾. For the estimation of skin-friction drag listed in the second part of Table 3, Morgan⁽²⁵⁾ again used flat plate turbulent boundary-layer data in conjunction with his estimates of surface wetted area. This procedure he applied to the wings (and wing engines), body (and nose engine), tail unit and undercarriage, struts and wires as appropriate.

As was usual in Britain by then, Table 3 lists the various drag contributions reduced to the drag in lbs at a speed of 100 ft/s at sea level. Morgan's detailed calculations of the various skin-friction contributions to profile drag result in slight changes to the data listed in Table 2. The Heinkel, in particular, emerges with an even higher cleanness ratio.

Table 3 Drag Contributions in lbs at 100 ft/s

Estimated Drag lbs at 100 ft/s	Heinkel He 70	Handley Page Harrow	Armstrong Whitworth Whitley	Hawker Hurricane Prototype	Gloster Gladiator
Engine Installation	6.8	50.0	57.0	10.0	15.4
Wings	27.8	104.0	121.0	23.5	32.8
Body & Cabin	17.2	80.0	62.5	11.3	14.5
Tail Unit	7.2	25.0	27.5	5.0	5.6
Excrescences	1.0	20.0	11.6	0.3	4.0
Undercarriage	4.0	63.9	9.7	0	17.5
Struts & Wires	0	4.0	1.4	0	6.9
Interference	1.0	12.0	9.0	2.0	4.0
Remainder	7.3	51.1	76.3	22.4	8.5
Total Residual Drag	72.3	410.0	376.0	74.5	109.2
Turbulent Skin Friction (Flat Plate)					
Wings + wing engines	24.4	71.5	83.3	16.2	23.2
Body + nose engine	11.1	42.0	29.0	5.94	6.5
Tail unit	6.0	20.1	22.0	3.98	4.5
Undercar, struts, wires	0.2	10.1	1.1	0	4.0
Total skin friction	41.7	143.7	135.4	26.12	38.2
Cleanness Ratio	0.576	0.35	0.36	0.35	0.35

Source: Morgan, Reference 25

In his assessments of the two aircraft having fixed undercarriages, the Harrow and the Gladiator, Morgan⁽²⁵⁾ noted that these features account for about 16% of the residual drag. However, he was particularly concerned with the item listed as 'Remainder' in Table 3. As a percentage of the total residual drag, this is particularly high for the Hurricane (30%), whereas for the Gladiator it is the least of the five at about 8%. He put this down to features the effects

of which were as yet not known but he suspected that surface irregularities together with leaks around access panels and, for the bombers, bomb doors were probable culprits. He recommended that the Hurricane be tested in the RAE's 24 ft Open Jet Tunnel so that more accurate data might be obtained. This was done and the detailed results proved most useful in Collar's investigation⁽²⁴⁾ two years later.

5.5 Thrust from exhausts and radiators and other improvements

A number of improvements in the assessment procedures appeared around this time. In 1935 Meredith⁽²⁶⁾ had introduced the idea of the ducted radiator for liquid-cooled engines and by 1937 Capon⁽²⁷⁾ had provided an analysis from which the additional thrust produced by radiator heat regeneration could be calculated. In March 1940 Hartshorn, Diprose and Patterson⁽²⁸⁾ provided an assessment of the thrust available from rearward-directed exhaust momentum. Thus the thrust augmentation produced by these two means could be added to the propeller thrust ($\eta P/V$) provided by the engine. As the total thrust is equal to the total drag in steady level flight at constant speed, a more accurate drag assessment could then be obtained from flight-test thrust results.

Thus far the method of boundary-layer drag estimation had relied on that introduced by Jones⁽¹⁸⁾, being based on flat plate turbulent boundary layer data. This was seen to be inaccurate as a predictor of boundary-layer drag since it took no account of velocity variations over an aeroplane's surfaces; in the flat plate case, such variations are absent. Moreover, it was realised that the boundary layer creates a form of drag additional to skin friction. This is caused by the slower moving boundary layer's gradual thickening as it develops over a surface. Thus the boundary layer 'shoulders aside', or outwardly displaces slightly, the flow exterior to it. The exterior flow 'sees' a body shape slightly thicker than the actual body, and this 'seen' body extends into the wake. The consequence is that the pressure at the trailing edge does not return to the value it would have reached had the boundary layer been absent and this creates the fore-and-aft pressure imbalance called boundary-layer pressure drag. Again this effect is absent in the case of the flat plate held at zero incidence, there being no streamwise force due to pressure on such a surface. Both of these deficiencies in the flat plate method were rectified in the turbulent boundary-layer analysis developed by Squire and Young⁽²⁹⁾ (Figures 7 and 8) in 1937, more details of which are given in Reference 2. The method gave good agreement with experiments on aerofoil sections and thus provided more reliable drag estimates for wings. By 1939 Young⁽³⁰⁾ had extended the method to bodies of revolution which could be applied to fuselages.

An important feature of the Squire and Young analysis⁽²⁹⁾ is that it shows a clear relationship between the additional boundary-layer pressure drag and a wing's thickness/chord ratio, t/c . Squire emphasised this feature in the discussion following Relf's lecture⁽³¹⁾ to the Royal Aeronautical Society in 1938. Young⁽³²⁾, in reviewing Reference 29's method, pointed out that a good approximation to its results is

$$(\text{Boundary-layer pressure drag})/(\text{Total boundary-layer drag}) \approx t/c. \quad (11)$$

The total boundary-layer drag is the sum of the skin-friction and pressure drags. Drawing on Reference 30's results, Young⁽³²⁾ added that for bodies of revolution, maximum diameter d and length ℓ , the effect is rather less:

$$(\text{Boundary-layer pressure drag})/(\text{Total boundary-layer drag}) \approx 0.4d/\ell. \quad (12)$$

These results, in conjunction with the CAT investigation into drag for aerofoils having higher t/c ratios mentioned in Section 4, corroborated Jones's belief⁽¹⁸⁾ that aerofoil drag increases with increasing thickness/chord ratio.

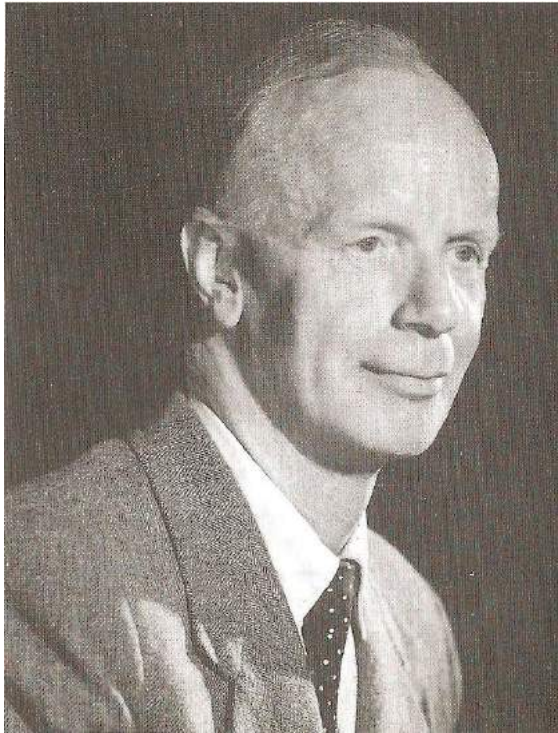


Figure 7 Herbert Brian Squire FRS (1909 – 1961). Copyright: Godfrey Argent Studio

Joining the Aerodynamics Department of the RAE in 1934, he moved to the Aerodynamics Division of the National Physical Laboratory in 1949. He became Zaharoff Professor of Aviation at Imperial College, London, in 1952.



Figure 8 Alec David Young FRS (1913 – 2005)
Source: Royal Aeronautical Society (National Aerospace Library)

He joined the Aerodynamics Department of the RAE in 1936, moving to the College of Aeronautics, Cranfield, in 1946. In 1950 he became Professor of Aerodynamics there and, in 1954, Professor of Aeronautical Engineering at Queen Mary College, University of London, until retirement in 1978.

5.6 Drag of the Spitfire and Hurricane

Two early beneficiaries of these advances in thrust and drag estimation were Hufton (Figure 9) and Collar (Figure 10). Hufton's report⁽³³⁾ of April 1940 compares the drag of a standard Spitfire with that of the High Speed Spitfire intended for an attempt at the Landplane World Speed Record. Collar's comparison⁽²⁴⁾ of the Spitfire and Hurricane emerged in June 1940

and its findings are described in detail in Section 3 of Reference 2. For ease of reference, Collar's data⁽²⁴⁾ are repeated in Table 4A for comparison with Morgan's Hurricane data⁽²⁵⁾ on the one hand and Hufton's Spitfire data⁽³³⁾ on the other.

As mentioned earlier, Morgan⁽²⁵⁾ included more detailed drag data for individual airframe parts which contributed to his subtotal categories listed in Table 3. These more detailed data have been re-assigned here in an attempt to make them fit the subtotal categories listed in Table 4A, the latter categories being those chosen by Collar⁽²⁴⁾ and Hufton⁽³³⁾. Even so,



Figure 9 Philip Arthur Hufton (1911 – 1974) Source: Farnborough Air Sciences Trust

He joined the Aerodynamic Flight of the RAE in 1934 and rose to be Deputy Director (Aircraft).

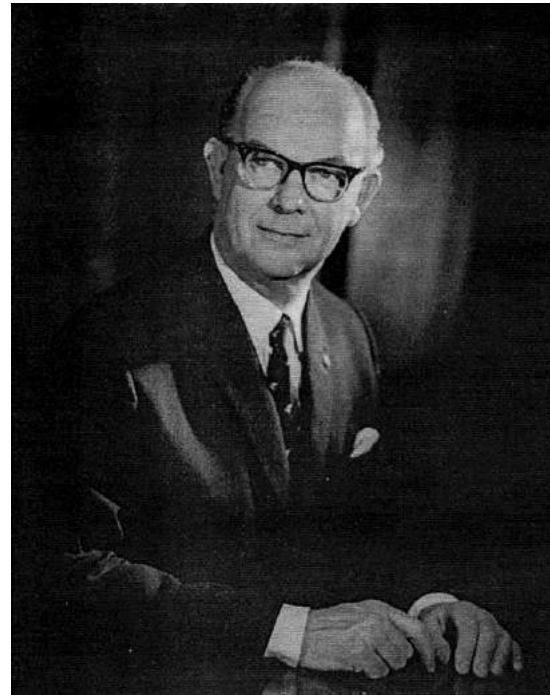


Figure 10 Arthur Roderick Collar FRS (1908 – 1986) Source: Royal Aeronautical Society (National Aerospace Library)[Royal Society] He joined the Aerodynamics Department of the National Physical Laboratory in 1929, transferred to the Structural and Mechanical Engineering Department of the RAE in 1940, there to work on aeroelasticity. In 1946 he became Sir George White Professor of Aeronautics at Bristol University until retirement in 1973

there are anomalies. For example, Morgan's item listed as Profile drag (wings, fuselage and tail) may have included Cooling Drag and Windscreen. As to Induced drag, this is unknown since Morgan's data⁽²⁵⁾ are for residual drag only. The various contributions to Thrust are also unknown, not having been listed in the original RAE report⁽²³⁾. However, it is known that the Hurricane prototype did not possess ejector exhausts so that a value of zero is given in that case. Similarly, the prototype had a retractable tailwheel so here again a zero value can be assigned. As to gun holes, the prototype lacked these but did possess an aerial post, so this might explain the difference between Morgan's assessment⁽²⁵⁾ and that by Collar⁽²⁴⁾ for

what was presumably an early production Hurricane. As to the high drag not accounted for by Morgan⁽²⁵⁾, about half of this could be what Collar⁽²⁴⁾ attributes to leaks.

It will be recalled that the data⁽²³⁾ on which Morgan⁽²⁵⁾ based his Hurricane assessment were suspected of having rather too high values for both engine powers and propeller efficiencies, but neglected to include radiator thrust. These, it is felt, may have cancelled each other out, the result being that Morgan's C_{D0} value is very close to that obtained from Collar's more detailed assessment⁽²⁴⁾ as shown in Table 4B. Morgan's CR and C_{D0} values quoted there, based on flat plate drag data, are those listed in Table 3. However, the corresponding values calculated from Collar's Hurricane assessment⁽²⁴⁾ are significantly higher, based as they are on the more accurate methods of Squire and Young⁽²⁹⁾ and Young⁽³⁰⁾. Broadly speaking, then, the aircraft assessed earlier were a good deal aerodynamically cleaner than the RAE had hitherto supposed.

Table 4A Thrust/Drag Contributions in lbs at 100 ft/s

	Hurricane Morgan ⁽²⁵⁾	Hurricane Collar ⁽²⁴⁾	Spitfire Collar ⁽²⁴⁾	Spitfire Hufton ⁽³³⁾	High speed Spitfire 1938 Hufton ⁽³³⁾
Thrust					
Engine/propeller thrust	?	73.0	51.5	52.15	44.95
Exhaust Thrust	0	9.0*	7.5*	6.35	6.75
Heat Regeneration Thrust	?			1.7	1.6
Total Thrust	?	82.0	59.0	60.2	53.3
Drag					
Induced drag (including washout)	?	4.0	3.0	3.0	1.2
Residual Drag					
Roughness (including rivets, joints, paint)	---	3.3	2.0	2.0	---
Cooling drag (including oil cooler)	---	8.0	7.0	7.0	6.0
Air intake	1.5	1.0	1.0	1.0	1.0
Tail wheel or skid	0	2.0	2.0	2.0	1.0
Tailplane protection	---	---	0.3	---	---
Gun holes, aerial post	0.3	0.8		0.8	0.7
Windscreen	---	1.5		1.2	
Leaks (including control gaps)	---	11.0	5.0	1.2	0.9
Wing-body interference	2.0	9.9	4.5	1.5	1.5
Not Accounted For	22.4	---	---	8.4	12.9
Total Drag	?	82.0	59.0	60.2	53.3
Total Residual Drag	74.5	78.0	56.0	57.2	52.1

* Exhaust & Heat Regeneration Combined

Neither Collar⁽²⁴⁾ nor Hufton⁽³³⁾ takes the further step of calculating C_{D0} but this has been done here and the results are given in Table 4B. Included are the values for CR and C_{D0} together with aspect ratio, A. For want of precise values for the factor k in equation (7), that equation is used merely to calculate $k^{1/2} (L/D)_{\max}$ and thereby provide an indication of the maximum lift to drag ratio.

Table 4B Derived Results

	Hurricane Morgan ⁽²⁵⁾	Hurricane Collar ⁽²⁴⁾	Spitfire Collar ⁽²⁴⁾	Spitfire Hufton ⁽³³⁾	High speed Spitfire 1938 Hufton ⁽³³⁾
Wing Span/ft	40	40	37	37	33.5
Wing Planform Area S/ft ²	264	264	242	242	232
Heat Regeneration Thrust	?			1.7	1.6
Aspect Ratio A	6.06	6.06	5.66	5.66	4.84
CR	0.35	0.52	0.58	0.56	0.54
C_{D0}	0.009	0.013	0.012	0.011	0.010
C_{D0}	0.025	0.025	0.020	0.020	0.019
$k^{1/2} (L/D)_{\max}$	13.8	13.8	14.9	14.9	14.1

Turning now to the Collar⁽²⁴⁾ and Hufton⁽³³⁾ data in Table 4A for the standard Spitfire, these are largely in agreement. As Collar⁽²⁴⁾ explains, a number of the minor items (Air intake, Tailwheel, Gun Holes) have been obtained from RAE tests on a Hurricane in the 24 ft Open Jet Tunnel and such features are sufficiently similar to those on the Spitfire to justify applying their results to that aircraft; presumably Hufton⁽³³⁾ took the same view. The main differences between the two assessments are that Collar⁽²⁴⁾ has higher Leak and Interference values but no Drag unaccounted for, whereas a value for the latter appears in Hufton's assessment⁽³³⁾. However, Hufton⁽³³⁾ allows that this item might be due to leaks but also to such other factors as propeller-body interference, compressibility loss, errors in performance measurements, thrust estimation and the boundary-layer transition point having been assumed to lie at wing leading edges and fuselage noses. The latter is also assumed by Collar⁽²⁴⁾ on the grounds that turbulence in the propeller wash will infect the fuselage and the inboard parts of the wing whilst gun holes will have a similar effect on much of the wings' outboard parts. A further slight difference between the two reports is that Collar⁽²⁴⁾ combines exhaust and radiator thrusts whereas Hufton⁽³³⁾ lists them individually. Indeed, his is even more detailed in that he provides corrections to engine power due to the back pressure of the ejector exhausts. These corrections have been obtained from simulated altitude tests at 18,500 ft on a Merlin II conducted by the RAE's Engine Department. That report, dated May 1939, shows that the power reduces from 1057 hp to 1033.5 hp. Martlesham Heath's report of January 1939 for flight tests with Spitfire K 9787 at the above altitude gives the maximum speed as 362.5 mph. This aircraft, K9787, is the first production Spitfire I⁽³⁴⁾. Collar⁽²⁴⁾ is less specific, stating a power of 1020 hp at 18,000 ft, at which altitude the maximum speed is 365 mph, the Hurricane's speed being 40 mph lower. For propeller efficiency, Hufton⁽³³⁾ provides a detailed assessment of losses for the twin-bladed wooden Vickers Jablo unit which results in a value for η of 0.77. In this respect, although Collar⁽²⁴⁾ has consulted Hufton's report⁽³³⁾, he opts for a η value of 0.8 but does not state the type of propeller used. As

mentioned earlier, these values for η call into question the accuracy of those higher values listed in Table 2 taken from earlier reports^(22, 23).

Nonetheless, Collar's and Hufton's C_{D0} values listed in Table 4B for the standard Spitfire are virtually identical and have very similar C_{D0} values. As to cleanness, the CR values are therefore closely similar and both slightly better than that for the Hurricane. Collar⁽²⁴⁾ points out that the Hurricane's higher Profile drag, 40.5 lbs compared with the Spitfire's 32.2 lbs, is not only due to its larger size and therefore greater wetted area but also to its wing's higher t/c ratio.

The mysterious item labelled Tailplane protection in Collar's assessment⁽²⁴⁾ has recently been investigated by Brinkworth⁽³⁵⁾. He concludes that this was probably a small guard fitted to the top of the fin, not the tailplane. Its purpose was to prevent the cable of an anti-spin parachute, if deployed in an emergency, slipping between the fin and the rudder and thus jamming the rudder.

Hufton's assessment⁽³³⁾ of the High Speed Spitfire is again meticulous, particularly with regard to thrust estimation. The aircraft has a much more powerful engine than the standard Spitfire and the RAE Engine Department has supplied him with power estimates at an altitude of 3,000 ft for three speeds, namely 300 mph, 350 mph and 400 mph. At the highest speed, and after corrections for exhaust back pressure, the power is estimated to be 1941 hp. The propeller is a Watts four-bladed fixed-pitch unit of smaller diameter than that used on the standard Spitfire which is therefore less prone to compressibility losses. For this Hufton⁽³³⁾ calculates a η value of 0.78. His drag estimates are calculated for all three speeds but his results for the 400 mph case only are listed in Table 4A for brevity's sake. At the lower speeds his results for Profile and Induced drags differ slightly. In the former case this is due to the boundary-layer drag obtained using References 29 and 30 varying with Reynolds number, the result being that the profile drag, when reduced to the 100 ft/s standard, decreases very slightly with increasing speed. As to Induced drag, this also reduces as speed increases because the aircraft flies at lower C_L values. Although the data of Table 4A show that a significant drag reduction has been achieved when compared to the standard Spitfire's results, 53.3 lbs compared with 60.2 lbs for Total drag, Table 4B shows that the reduction in C_{D0} is small. This is partly due to the fact that, whilst drag is reduced, so too is the planform area S.

At first sight it appears odd, perhaps even erroneous, that Hufton's Engine/propeller thrusts (Table 4A) turn out to be higher for the standard Spitfire than for the High Speed Spitfire when the latter clearly has a far more powerful engine. This is resolved, however, when account is taken of Appendix 2's procedure used to reduce flight data at high speed and altitude to sea-level conditions at a speed of 100 ft/s. Equation (A2.10) is the engine-thrust reduction relation and the crucial term there is $P/(\sigma V^3)$. The power P increases from 1033.5 hp (standard Spitfire) to 1941 hp (High Speed Spitfire) whereas the increase in V from 362.5 mph to 400 mph, even when cubed, is far less of a compensatory increase. A far larger effect, however, is produced by the density ratio $\sigma = \rho/\rho_0$, ρ_0 being the sea level air density. For the standard Spitfire at 18,500 ft $\sigma = 0.56$ whereas for the High Speed Spitfire at 3,000 ft

$\sigma = 0.92$. It is largely due to σ 's influence appearing in the denominator of $P/(\sigma V^3)$ which compensates for the lower P of the standard Spitfire and thus results in its higher Engine/propeller thrust recorded in Table 4A.

Before leaving the Collar⁽²⁴⁾ and Hufton⁽³³⁾ assessments, it is interesting to compare their results with those which would have been obtained using Loftin's approach⁽⁵⁾ in which thrust augmentation effects are ignored. Using Collar's Hurricane data in Table 4A as an example, according to Loftin's method the thrust would be solely 73 lbs and this would be taken to be the total drag. Deducting the Induced drag of 4 lbs leaves a Residual drag of 69 lbs, not Collar's value of 82 lbs, and this would yield the lower C_{D0} value of 0.021. This exercise applied to Collar's Spitfire data gives the lower value of 0.017. Thus the Loftin⁽⁵⁾ approach for cases in which thrust augmentation is significant underestimates C_{D0} by about 15%.

By 1940 the RAE's drag assessment method had reached a reasonably high level of accuracy. Notably in Hufton's case⁽³³⁾, this had resulted in a data layout similar to an accountant's company balance sheet. On the Credit side, engine thrusts corrected for back pressure and propeller efficiency could be added to thrusts provided by the exhausts and ducted radiators so as to provide reasonably accurate values for total thrust. That total Credit must then be balanced against the Debit total produced by the various forms of drag. Prediction of the latter had improved significantly with the use of the Squire and Young⁽²⁹⁾ and Young⁽³⁰⁾ profile drag analyses and the increasing amounts of more accurate wind tunnel data for various contributors to parasite drag.

5.7 Drag of bombers

All this was put to use by Bottle⁽³⁶⁾ in his RAE report of November 1940 which assessed bomber performance. The aircraft assessed are the Avro Manchester (both 80 ft and 90 ft span versions), Handley Page Halifax, Short Stirling, Douglas DB 7 (Boston in RAF service), Glen Martin 167 (Maryland in RAF service), Heinkel He. 111 and Junkers Ju. 88. For comparison, Bottle⁽³⁶⁾ also includes recent data for the Vickers Wellington 1A, Handley Page Hampden and Armstrong Whitworth Whitley. The newer British aircraft, the two Manchesters, Halifax and Stirling, are all prototypes and therefore probably not representative of subsequent Service aircraft. For example, Bottle⁽³⁶⁾ states that the 90 ft span Manchester has the turrets faired. All four aircraft had been tested by the A&AEE in 1940 after its move at the war's outbreak from Martlesham Heath near the East Coast to the safer location of Boscombe Down near Salisbury. The A&AEE's tests of the Glen Martin 167 were not yet complete. Flight-testing of the other British aircraft, and probably the Douglas DB 7, had been conducted at Martlesham Heath. There were no British performance tests available for the two German aircraft. The Heinkel, Bottle⁽³⁶⁾ believes, was a standard aircraft, presumably a captured example although it is unclear if it was in a flyable condition. As to the Junkers, Bottle⁽³⁶⁾ comments dryly that "no complete machine was available for inspection". His further purpose with the two German aircraft and the Glen Martin was not only to provide drag assessments but also to use their data to estimate maximum speed, the latter being unknown.

Bottle's thrust and drag data⁽³⁶⁾ for the four newer British aircraft are given in Table 5A. Table 5B shows the data for the two American and the two German aircraft. In both tables only the total Engine installation data are given whereas Bottle⁽³⁶⁾ lists individual drag items such as those due to air intakes, exhausts and coolers both internal and external. The drag item labelled Roughness is due to camouflage paint. For the British aircraft, the propellers are de Havilland constant speed units, the metal blades being of thin section, and for these units Bottle⁽³⁶⁾ takes η to be 0.82 whereas for the others $\eta = 0.8$ is assumed.

Table 5A Thrust/Drag Contributions in lbs at 100 ft/s

	Manchester (span 80 ft) 1939	Manchester (span 90 ft) 1940	Halifax 1939	Stirling 1939
Thrust				
Engine/propeller thrust	353	396	450	537
Exhaust Thrust	21	22.5	20	18.5
Heat Regeneration Thrust	6.5	7	8	0
Total Thrust	380.5	425.5	478	555.5
Drag				
Induced drag	65	75	38	83
Residual Drag				
Wings: Profile drag	96	106	127	131.5
Roughness	14	16	24	26
Controls	7	7	7	9
L. E. slats	---	---	15	---
Fuselage: Profile drag	36	36	37.5	46
Roughness	2.5	4.5	3	3
Cabin	2	2	2	
Rear turret	19	17	17	19
Front turret	3	3	3	3
Tail: Profile drag	26	26	30.5	26.5
Extra fin	2	2	---	---
Roughness	7	7	6	5.5
Controls	8	8	7	11
Wing-fuselage interference	5	5	5	5
Engine installation		59	59	100
Miscellaneous: Wireless mast(s)	2	2	3	1.5
Pitot		0.5 0.5	1	0.5
Small protuberances	8	8	5	---
Leaks		20	20	18
Not Accounted For	-1.5	21.5	29	57
Total Drag	380.5	425.5	478	555.5
Total Residual Drag	315.5	350.5	440	472.5

Source: Bottle, Reference 36

Table 5C lists C_{D0} and cleanliness ratio CR for all of the aircraft considered in Bottle's report⁽³⁶⁾. Here the CR values are those obtained using the boundary-layer profile drag analyses of References 29 and 30. In his report, Bottle⁽³⁶⁾ adds values based on the older flat plate analysis though these are not included here. The bomber C_{D0} values are higher than those for the fighters given in Table 4B due to the larger amounts of parasite drag created by engine nacelles, gun turrets and such. Consequently, the CR values are smaller. Using the values for C_{D0} and aspect ratios, A, in conjunction with equation (7), values for $k^{1/2} (L/D)_{max}$ have been calculated and are listed in Table 5C. The two American aircraft, Boston and Maryland, benefit here due to lower C_{D0} values and higher aspect ratios.

Table 5B Thrust/Drag Contributions in lbs at 100 ft/s

	Douglas DB 7 (1939)	Martin 167 (1939)	Heinkel He. 111H (1939)	Junkers Ju. 88A (1938)
Thrust				
Engine/propeller thrust	141	156	268.5	251.5
Exhaust Thrust	0	0	0	2.5
Heat Regeneration Thrust	---	---	3.5	---
Total Thrust	141	156	272	254
Drag				
Induced drag	7	9.5	31.5	46
Residual drag				
Wings: Profile drag	43	46.4	79.5	48
Roughness	3	3.7	8.5	4
Controls	3	2	4	7
Fuselage: Profile drag	14	12.6	22.5	16
Roughness	1	0.9	2	1
Cabin	4	4	2	6
Upper turret/rear cockpit	---	3	15	---
Lower gun position	---	4	9	6
Tail: Profile drag	14	13.7	20	14
Roughness	1	1.1	2.5	1
Controls	3.5	3	6	4
Wing-fuselage interference	2	4	2	5
Engine installation	36	36	51	48
Miscellaneous: Wireless mast(s)	0.5	1.2	1.5	1.5
Pitot	0.5	0.5	1	0.5
Small protuberances	1	4	3	6
External bombs	---	---	---	32
Leaks	8	6.4	12.5	8
Not Accounted For	-0.5	0	0	0
Total Drag	141	156	272	254
Total Residual Drag	134	146.5	240.5	208

Source: Bottle, Reference 36

Table 5C Zero lift drag coefficients and cleanness ratios

	C_{D0}	Cleanness ratio CR	Aspect ratio A	$k^{1/2} (L/D)_{max}$
Avro Manchester (80 ft)	0.0255	0.51	6.15	13.8
Avro Manchester (90 ft)	0.0265	0.49	7.28	14.7
Handley-Page Halifax	0.0293	0.45	7.76	14.4
Short Stirling	0.0266	0.44	6.70	14.1
Vickers Wellington 1A (1936)	0.0291	0.45	8.84	15.4
Handley-Page Hampden (1936)	0.0271	0.48	6.95	14.2
Arm. Whit. Whitley	0.0259	0.46	6.21	13.7
Heinkel He 111	0.0220	0.51	5.90	14.5
Junkers Ju 88	0.0320	0.38	6.51	12.6
Douglas DB 7 (Boston)	0.0243	0.53	8.09	16.2
Martin 167 (Maryland)	0.0232	0.50	11.40	19.6

Source: Bottle, Reference 36

It will be recalled that Bottle⁽³⁶⁾ had no flight-test performance data for the Martin 167 Maryland and the two German aircraft but one purpose of his investigation was to estimate their maximum speeds. However, it is not entirely clear how he achieved this. It may be that he used his assessment procedure in reverse, so to speak. Using the analyses of References 29 and 30 and the known geometries of the aircraft, together with reasonable estimates for their flight Reynolds numbers, he would be able to estimate profile drag. He would also have sufficient data to make reasonable estimates of the parasite drag contributions listed in Table 5B. The resulting estimate for the total drag must then be equal to the total thrust. The latter is then corrected for thrust augmentation effects and propeller efficiency (η he assumes to be 0.8). The engine thrust can then be calculated and from the engine's maximum power, which is known, an estimate for the maximum speed follows. His maximum speed estimates are listed in Table 5D together with published performance data for the three aircraft. However, there is a difficulty with regard to the latter in that their stated altitudes do not match those chosen by Bottle⁽³⁶⁾. The published data chosen here are those which this author has to hand and provide the closest match to Bottle's altitudes. For the Martin 167, data⁽³⁷⁾ for the RAF's Maryland I are given in Table 5D. For the Heinkel, Bottle⁽³⁶⁾ states that the engines are Jumo 211D units. This suggests that the Heinkel variant is the 111H with the glass-nosed cockpit⁽³⁸⁾ and it is its maximum speed which is listed in Table 5D. As to the Junkers, this has Jumo 211B engines suggesting the 88A variant, data⁽³⁸⁾ for which are also given in the table. Comparison of these results suggests that Bottle's estimates are reasonably accurate. The biggest difference is that for the Junkers, but it must be pointed out that for this aircraft Bottle⁽³⁶⁾ includes in the data of Table 5B the drag of six 250 kg bombs carried externally, a drag addition which contributes about 13% to the total.

Table 5D Estimated maximum speeds

	Bottle ⁽³⁶⁾	Cooper and Thetford ⁽³⁷⁾	Green ⁽³⁸⁾
Martin 167 Maryland	297 mph @ 10,000 ft	298 mph @ 7,500 ft	
Heinkel He 111H	254 mph @ 13,000 ft		255 mph @ 13,120 ft
Junkers Ju. 88A	266 mph @ 15,000 ft		280 mph @ 18,050 ft

5.8 Collected drag and thrust data

As the war years progressed and more new aircraft entered British service, performance data obtained at Boscombe Down and at the RAE itself were passed to the RAE's Aerodynamics Department. When analysed there, these yielded a considerable quantity of basic aerodynamic data. These the RAE began to issue in reports covering both aerodynamic and structural data for the aircraft assessed. This was a joint effort by the Aerodynamics Department and the Structural and Mechanical Engineering Department (SME). The SME's interest was in assessing various structural efficiency factors, an exercise which deserves a survey in its own right. Here, however, we are interested only in the Aerodynamics Department's assessment of drag, particularly with regard to the estimation of C_{D0} using the methods used by Hufton⁽³³⁾ and Bottle⁽³⁶⁾ described above.

The first issue of the report⁽³⁹⁾, although undated, probably appeared in 1942. An addendum of January 1943 corrected data for the Halifax. In November 1943 Issue 2 of the report appeared, stating an intention to provide updates at intervals of six months to one year. Issue 3 appeared in August 1945, an addendum was added in October of that year giving data for three British jet aircraft and this was followed by a further addendum in April 1946 correcting and adding further data.

As an indication of the detail provided by Reference 39, Table 6 lists the drag data for five sample aircraft. Here, and in all cases listed in that reference, for simplicity the induced drag has been estimated using equation (5) with $k = 1$.

With regard to the Mustang III's low C_{D0} value compared with that for the Spitfire IX, both aircraft have similar totals for Profile Drag, 29.4 lbs (Mustang) and 29.9 lbs (Spitfire), whereas Power Plant Drag and Guns are significantly less for the Mustang. Since Power Plant Drag includes cooling drag, it may be, as suggested in Reference 2, that the Mustang benefits here from the greater area ratio of its radiator duct which reduces the drag of its radiator matrix. As to Guns, the Mustang is stated to have had its 0.5 in machine gun ports sealed whereas this was not the case for the cannon-armed Spitfire. Under the Miscellaneous heading, the Mustang again benefits from its fewer excrescences. The Spitfire's high value for Drag Not Accounted For may be due, in part, to overestimation of Propeller Thrust. In this respect, Issue 3 (August 1945) of the report⁽³⁹⁾ stresses that the accuracy with which C_{D0} is obtained from flight tests depends entirely on the accuracy of the estimation of engine power. It feels that a thrust or torque meter would be a great asset in improving the accuracy of C_{D0} determination, an indication that there was some doubt as to engine thrust accuracy.

It will be recalled that Loftin's method⁽⁵⁾ ignores thrust augmentation and for the P-51D he gives a C_{D0} value of 0.0163. Applying that method to the Mustang III data of Table 6, the residual drag of 48.8 lbs is replaced by 41.1 lbs. The latter yields $C_{D0} = 0.0148$, an underestimation similar to that quoted for this method's application earlier to Collar's Spitfire data⁽²⁴⁾. However, the Mustang III and the P-51D are not strictly comparable. The Mustang III's nearest American equivalent is the P-51B/C variant, not the P-51D which introduced the lower rear fuselage decking and bubble cockpit hood providing better all-round vision.

The maximum speed tests on both the Spitfire IX and the Mustang III had initially been conducted at altitudes around 26,000 ft, conditions which yielded higher values for C_{D0} . Reference 39 states the suspicion that such high-speed tests were encountering compressibility effects even in straight and level flight. Therefore the tests were repeated at altitudes close to sea level at which maximum speeds were lower and the sound speed higher, the resulting C_{D0} values being noticeably reduced. The above suspicion is confirmed by the author's calculations indicating that the high altitude tests were conducted at Mach numbers around 0.65. Mair's report of 1950⁽⁴⁰⁾ (see Figure 5 of Reference 2) on high subsonic flight tests at the RAE shows that compressibility effects causing higher values for C_{D0} were indeed encountered at these conditions. Therefore only the lower altitude test data for such cases are quoted in Tables 6 and 7.

The Sunderland V is the only aircraft listed in Table 6 which is powered by radial engines. In Reference 39 it was recognised that the interior ducting of such engine cowlings would produce heat regeneration thrust in similar fashion to that of a liquid-cooled engine's ducted radiator. In estimating this effect for aircraft with radial engines Capon's analysis⁽²⁷⁾ for ducted radiators was again used but thrust results were multiplied by an efficiency factor of 0.8.

The data for the multi-engine aircraft of Table 6, Mosquito, Lancaster and Sunderland, illustrate the consequences for Power Plant Drag inherent to such aircraft. For the two four-engine aircraft there are additional drags due to gun turrets. Such unavoidable consequences of their mission requirements lead inevitably to higher C_{D0} values and lower cleanliness ratios.

All of the C_{D0} and other data from the various issues of the report⁽³⁹⁾ are brought together in Table 7. However, in Issue 2 of November 1943 the cleanliness ratio (CR) results were dropped from the report's data tables. The author has calculated these quantities from the detailed data in this and subsequent tables, the results being given in italics. Included in Table 7 are the author's calculations for $k^{1/2} (L/D)_{\max}$ using equation (7), the results again being given in italics.

The data in Table 7 are grouped in the categories adopted in Reference 39: single engine fighter, single engine fighter (naval), twin engine fighter, naval torpedo & light bomber, twin engine bomber, four engine heavy bomber, flying boat.

Table 6 Thrust/Drag Contributions in lbs at 100 ft/s

	Spitfire IX	Mustang III	Mosquito	Lancaster	Sunderland
Propeller Thrust	65.0	43.0	138.2	492.0	610.0
Exhaust Thrust	7.5	6.6	22.7	69.0	58.4
Heat Regeneration Thrust	1.4	1.1	4.4	7.0	4.4
Total Thrust	73.9	50.7	165.3	568.0	627.8
Induced Drag	1.4	1.9	9.8	79.2	84.0
Profile Drag Wings	19.0	17.5	39.6	116.9	147.0
Profile Drag Body	6.8	7.0	12.3	31.4	106.3
Profile Drag Tail	4.1	4.9	14.1	29.4	37.8
Power Plant Drag	15.7	13.4	32.6	100.0	85.6
Guns & Turrets	5.0	0	2.1	64.5	43.5
Radio	0.5	0.6	1.0	13.2	30.5
Roughness	1.2	1.2	11.3	19.2	31.4
Misc. Incl. Control Gaps	9.9	6.0	15.1	66.7	67.3
Drag Accounted For	62.2	50.6	128.1	441.3	549.4
Drag Not Accounted For	10.3	-1.8	27.4	47.5	39.4
Total Residual Drag	72.5	48.8	155.5	488.8	588.8
Cleaness ratio (CR)	0.412	0.603	0.424	0.364	0.494
C_{D0}	0.0252	0.0175	0.0273	0.0316	0.0293

Source: RAE Staff, Reference 39

Table 7 Drag and other data for a variety of types

	C_{D0}	Cleaness ratio CR	Aspect ratio A	$k^{1/2} (L/D)_{max}$
Single Engine Fighter				
Hurricane I	0.0249	0.534	6.2	14.0
Hurricane II	0.0253	0.516	6.2	13.9
Hurricane IV	0.0307	0.413	6.2	12.6
Spitfire Vb	0.0213	0.518	5.6	14.4
Spitfire Vc	0.0218	0.508	5.6	14.2
Spitfire IX	0.0252	0.412	5.6	13.2
Spitfire XXI (Prototype)	0.0182	0.521	5.6	15.5
Typhoon I (Prototype)	0.0216	0.564	6.2	15.0
Typhoon I	0.0238	0.540	6.2	14.3
Tempest II	0.0185	0.565	5.6	15.4
Tempest V (Prototype)	0.0199	0.563	5.6	14.9
Mustang I	0.0179	0.624	5.9	16.1
Mustang III	0.0175	0.603	5.9	16.3
Mustang X	0.0227	0.519	5.9	14.3
Fw 190A3	0.0279	0.444	6.0	13.0
Single Engine Fighter (Naval)				
Firefly III	0.0308	0.418	6.0	12.4

Firebrand	0.0228	0.587	6.7	15.2
Seafire IIc	0.0254	0.441	5.6	13.2
Seafire III	0.0235	0.460	5.6	13.7
Hellcat	0.0267	0.507	5.5	12.7
Twin Engine Fighter				
Whirlwind (Prototype)	0.0315	0.408	8.1	14.2
Welkin I	0.0297	0.449	10.6	16.7
Mosquito IIF	0.0226	0.488	6.1	14.6
Mosquito NF X	0.0258	0.527	6.1	13.6
Mosquito NF XV	0.0273	0.424	6.1	13.2
Beaufighter I	0.0272	0.440	6.6	13.8
Beaufighter IIF	0.0266	0.450	6.6	14.0
Naval Torpedo & Light Bomber				
Barracuda (Prototype)	0.0321	0.484	6.1	12.2
Barracuda II	0.0312	0.465	6.1	12.4
Beaufighter TF X	0.0354	0.349	6.7	12.2
Firebrand TF III	0.0281	0.436	6.8	13.8
Avenger I	0.0210	0.583	6.0	15.0
Twin Engine Bomber				
Buckingham (Prototype)	0.0232	0.516	7.3	15.7
Mosquito XVI B	0.0294	0.395	6.1	12.8
Mosquito IX B	0.0252	0.459	6.1	13.8
Boston III A	0.0296	0.429	8.1	14.7
Mitchell II	0.0258	0.476	7.4	15.0
Ju 88C6	0.0315	0.378	7.4	13.6
Four Engine Heavy Bomber				
Halifax I	0.0400	0.344	7.8	12.4
Halifax II	0.0365	0.357	7.8	13.0
Halifax III	0.0344	0.399	7.8	13.3
Lancaster I	0.0302	0.396	8.0	14.4
Lancaster II	0.0335	0.369	8.0	13.7
Lancaster III	0.0316	0.364	8.0	14.1
Lancaster VI	0.0333	0.344	8.0	13.7
Lincoln I	0.0324	0.364	10.1	15.6
Stirling	0.0314	0.374	6.7	13.0
Fortress II A	0.0253	0.467	7.6	15.4
Liberator III A	0.0407	0.355	11.7	15.0
Flying Boat				
Lerwick	0.0346	0.469	7.5	13.4
Sunderland I	0.0304	0.470	7.5	13.9
Sunderland II	0.0314	0.456	7.5	13.7
Sunderland III	0.0307	0.466	7.5	13.9
Sunderland V	0.0293	0.494	7.5	14.2
Mariner	0.0299	0.518	9.9	16.1

Source: RAE Staff, Reference 39

The first issue of Reference 39 remarks that the drag of a production aircraft is usually higher than its prototype. As an example, it points to the Typhoon data of Table 7. The report adds that the drag of production aeroplanes alters during the life of the type, generally increasing with time due to changes in operational equipment, engine developments and so on. This can be seen in Table 7's Merlin-powered Lancaster I, III and VI sequence (the Lancaster II was Hercules-powered) as the aircraft acquired more parasite drag creating features such as the blister housing H₂S radar. Surprisingly, however, the reverse is the case with the Merlin-powered Halifax I and II; the Halifax III was Hercules-powered. The effect of change in armament is shown in Table 7's high C_{D0} value for the Beaufighter TF X compared with that for the fighter version, Beaufighter IIF. On test the Beaufighter TF X carried an 18 in Mk. XII torpedo and the aircraft had been fitted with dive brakes which, when retracted, remained proud of the wings.

6. The Early Jet Age

6.1 Straight wing jet aircraft

The addendum to Issue 3 of Reference 39, dated October 1945, provides test-flight data for the Gloster E.28/39 and also for an interim version of the Gloster Meteor I and the De Havilland Vampire. The Gloster E.28/39 is the first British jet aircraft and its evolution is described in exemplary detail by Brinkworth⁽⁴¹⁾. In April 1946 the data for all three aircraft were incorporated in the final addendum's complete data sheet. For the three aircraft the thrust and drag estimates taken from that data sheet are given in Table 8. The engines are stated to be Rolls-Royce W2B/23/101 (E.28/39), Rolls-Royce W2B/23-C (Meteor) and De Havilland Goblin I (Vampire). For the E.28/39 a 4% loss of thrust is assumed due to the length of the jet pipe.

As noted at the end of Table 8, a correction applies to the C_{D0} value for the Vampire. The copy of the report⁽³⁹⁾ seen by the author carries the following hand-written explanation: "This drag figure includes some compressibility drag. RDT.1 and De Havilland both deduce at low Mach numbers a profile drag of about 44 lb at 100 ft/s [$C_{D0} = 0.0142$]." "Profile drag" here refers to the item labelled Total Residual Drag in Table 8.

Table 8 shows that the adoption of the jet engine resulted in significant drag improvements. There are now fewer parasite drag creating features, items associated with cooling for piston engines having been removed. Such improvements are seen to result in higher values for CR. However, of the two fighters, the Meteor benefits the least due to its twin-engine layout.

Drag results at low and high altitudes supplied by English Electric for the Canberra B.1 (1949) were analysed by the Aerodynamic Staff⁽⁴²⁾ in December 1950. It must be stressed that the flight test data were obtained at a Mach number of 0.74. Nonetheless, the low C_{D0} values given in Table 9 at this fairly high subsonic condition are remarkable. For lower speeds clear of compressibility effects they can be expected to be even lower and it would be interesting to know what they are. The results have been included here since they illustrate how much lower C_{D0} could become as the jet age progressed. For the Martin B-57B, the American version of the Canberra with extended wings, Loftin⁽⁵⁾ gives $C_{D0} = 0.0119$ at an

altitude of 2,500 ft and $M = 0.79$. The purpose of the RAE report⁽⁴²⁾ is to use the data in an attempt to estimate boundary-layer transition position on the wings; in this respect the assessment is rather inconclusive and further investigation is recommended.

Table 8 Thrust & Drag Contributions in lbs at 100 ft/s

	Gloster E.28/39 (1941)	Meteor I (1943)	Vampire (1943)
Engine Thrust	31.6	74.9	48.0
Induced Drag	0.8	2.1	1.7
Profile Drag Wings	9.8	23.6	17.7
Profile Drag Body	7.6	9.9	10.2
Profile Drag Tail	4.6	9.0	6.0
Power Plant Drag	0	13.0	2.0
Guns	0	1.2	1.6
Radio	0.3	0.3	0.3
Roughness	1.0	1.7	0.9
Misc. Incl. Control Gaps	5.9	8.9	5.4
Drag Accounted For	29.2	67.6	44.1
Drag Not Accounted For	1.6	5.2	2.2
Total Residual Drag	30.8	72.8	46.3
Cleaness ratio (CR)	0.714	0.584	0.732
C_{D0}	0.0174	0.0163	0.0150*

* Handwritten Correction 0.0142

Source: RAE Staff, Reference 39

Table 9 Drag of the English Electric Canberra B.1 at $M = 0.74$

Reynolds number	$Re = 22.5 \times 10^6$	$Re = 60 \times 10^6$
Altitude (ft)	40,000	10,000
C_{D0}	0.0119	0.0107

Source: RAE Staff, Reference 42

6.2 Swept wing jets

By 1950 Britain had adopted swept wings for its high speed aircraft. In December of that year, an RAE report by Courtney⁽⁴³⁾ compared the low-speed drag characteristics of two such British aircraft with those for the North American F-86A Sabre. The two British aircraft are the Supermarine E.41/46 (Supermarine 510) and the Hawker E.38/46 (Hawker P.1052). The Supermarine aircraft was a development of the straight-winged Attacker, to which swept wing and tail surfaces were fitted. It retained the Attacker's 'elephant-ear' intakes at the forward sides of the fuselage, its rear jet pipe and tailwheel undercarriage. The Hawker aircraft was a swept-winged development of the straight-winged Sea Hawk but retained that

aircraft's unswept tail surfaces together with its intakes at thickened wing roots, twin jet pipes at the trailing edge roots and nose-wheel undercarriage.

In the past, drag assessment based on flight-test results⁽³⁹⁾ had usually used engine power/thrust data at one known speed and altitude to determine the total drag coefficient C_D . An estimate for the induced drag coefficient C_{Di} had then been deducted to obtain the residual drag coefficient, the zero-lift coefficient C_{D0} . For the three swept-wing aircraft of Courtney's report⁽⁴³⁾ a new method had been used. In this the aircraft had been flown at a number of C_L values for which the corresponding values of the total drag coefficient, C_D , could be deduced. As to the latter, Courtney⁽⁴³⁾ states that the RAE's Aero Flight Section estimated that, given the jet pipe pressure and temperature and an accurate test-bed calibration of the engine, its thrust should be correct to within 2%. Thus a reasonably accurate value for the total drag, and hence C_D , can be determined from the flight-test thrust results. According to equations (5) and (6), a graph of $C_D \sim C_L^2$ should yield a straight line variation which, on extrapolation to $C_L = 0$, yields a value for C_{D0} . A further benefit of this approach is that the gradient of this graph yields a value for the induced drag factor k of equation (5). This method therefore not only avoids the need to estimate induced drag but also gives a value for k .

As Courtney⁽⁴³⁾ points out, there is, however, a difficulty with this approach. Flight at different C_L values entails flying at different speeds and therefore at different Reynolds numbers, Re . Profile drag and the other drag contributions are sensitive to Re , as illustrated by the Canberra results⁽⁴²⁾ above. As mentioned in Section 5, Hufton⁽³³⁾ had also encountered this problem of sensitivity to Reynolds number (Re) in estimating the drag of the High Speed Spitfire at three different speeds. Consequently, the resulting $C_D \sim C_L^2$ graph is not the desired straight line but one which is slightly curved. As Courtney⁽⁴³⁾ explains, a straight line can be chosen through the data points of the graph, in which case the value of C_{D0} obtained will correspond to some mean value of Re , and the value of k will also include the effect of Re variation. Here it is worth adding that in wind tunnel testing, in contrast, this difficulty can be avoided by using the same tunnel speed for all the tests at different C_L values (see below). The problem here, however, is the familiar one of wind-tunnel testing: the consequent fixed Reynolds number is much less than that at full scale.

Commenting on the three aircraft's drag coefficients derived using this method, Courtney⁽⁴³⁾ states that experience has shown that the uncertainty in determining C_{D0} from flight tests usually exceeds the uncertainty of 2% within which the thrust can in theory be determined. In view of the uncertainty regarding Re effects and the choice of the best curve through the scattered experimental points, he suggests that an inaccuracy of as much as 5% may well arise. His results for C_{D0} are given in Table 10A. From these Courtney⁽⁴³⁾ obtains the values for $D_{0,100}$, the drag in lbs at a speed of 100 ft/s at sea level conditions.

Table 10A Drag of swept wing aircraft

	C_{D0}	$D_{0,100}$ (lbs at 100 ft/s)
Supermarine E.41/46 (1948)	0.0164	53.5
Hawker E.38/46 (1948)	0.014	43.0
North American F-86A (1947)	0.013	44.5

Source: Courtney, Reference 43

The account sheet drawn up by Courtney⁽⁴³⁾ for estimates of the various drag contributions to match the total $D_{0,100}$ is shown in Table 10B. These contributions have been obtained using the analyses developed earlier⁽³⁹⁾. The item labelled ‘Chute housing’ for the E.41/46 refers to the housing for an anti-spin parachute, a feature absent on the other aircraft.

Table 10B Residual Drag, lbs at 100 ft/s

	Supermarine E.41/46	Hawker E.38/46	North American Sabre F- 86A
Wing			
Profile	18.85	15.5	18.45
Roughness	0	0	0
Control Gaps	0.95	0.8	0.90
Tail			
Profile	5.85	5.0	6.0
Roughness	0.05	0.05	0.05
Control Gaps	1.45	1.25	1.5
Body			
Profile	12.65	10.45	12.1
Roughness	0	0	0
Cabin	2.0	2.0	2.0
Miscellaneous			
Intakes	4.0	2.0	1.0
Exit	0.5	0.5	0.5
Interference	2.0	1.5	1.5
Pitot	0.5	0.5	0.5
‘Chute Housing’	0.5	---	---
Wheel Well		1.0	---
Total Accounted For	50.3	39.55	44.5
Total (Table 10A)	53.5	43.0	44.6
Unaccounted For	3.2	3.45	0.1
Unaccounted For %	6.0	8.0	0.2

Source: Courtney, Reference 43

Courtney⁽⁴³⁾ judges that, so far as the comparison between flight test and estimated drags is concerned, the unaccounted-for terms, of between zero and 8% of the total, indicate satisfactory agreement. On past aircraft, mainly piston-engine, the unaccounted-for term is

on the average about 9% of the total residual drag, and he suggests that a similar percentage may be found on jet aircraft. This he considers to show fairly good agreement between estimated and flight-test figures having regard to the order of accuracy that can reasonably be expected in estimating or measuring drag.

Courtney⁽⁴³⁾ provides interesting comments on the finish of the two British aircraft. He feels that the finish on the Supermarine is poor, the wing surfaces being, as he puts it, “somewhat rough and there were several poor panel junctions. Some rivets were not properly filled and others were not flush”. However, he excuses this on the grounds that it was designed and built in a hurry, not so much to achieve high-speed flight but rather to acquire experience of swept-wing flight as quickly as possible. As to the Hawker, no examination could be made at the time since it had recently crashed. However, from memory he judged it to have had a better finish, a judgement supported by his examination of the earlier Sea Hawk and the later Hawker P. 1081 with swept tail surfaces and straight-through jet pipe. As to the F-86A, he remarks that no example was yet available for inspection in Britain. His judgement is therefore based on published accounts from which he merely notes that these show wing leading-edge slats extending over most of the wing span, indicating a rather limited assessment.

Commenting on the various intakes used on the three aircraft, Courtney⁽⁴³⁾ judges that the fuselage side intakes of the Supermarine are generally less efficient on the whole than the body-nose or wing-root intakes used on the other two.

Courtney⁽⁴³⁾ concludes with a lengthy and detailed appendix surveying the current state of drag prediction. His opening paragraph is worth quoting in full.

“Drag estimation is by no means an exact science. It is based partly on theoretical calculations for ideal shapes of wings and bodies, partly on such wind tunnel and flight tests as are available on actual shapes, excrescences, leaks, roughness etc., and partly on past experience in comparing estimated total drags with those deduced from flight performance measurements. There is plenty of scope for error in the assumptions that have to be made, eg. on the amount of laminar flow existing in flight, or on the general standard of cleanliness – roughness of paint, amount of leakage, interference and so on.”

On wing profile drag Courtney⁽⁴³⁾ notes that this is estimated from the theoretically derived data provided by the Squire and Young⁽²⁹⁾ method, which was conveniently summarised in the Royal Aeronautical Society’s Data Sheets. Here it must be added that, during the war years, the Society had established a Technical Department, its aim being to bring together technical information from all available sources. Subsequently this became a separate entity, the Engineering Science Data Unit (ESDU). Courtney⁽⁴³⁾ points out that the Squire and Young method⁽²⁹⁾ was devised to deal with the earlier RAF and NACA aerofoil sections and probably needed updating to cope with the high-speed sections now being used.

Commenting on fuselage profile drag, Courtney⁽⁴³⁾ notes that assessments are based on Young’s method⁽³⁰⁾ which assumes an axially-symmetric body whereas few fuselages are of

circular cross-section; some errors can therefore be expected in this connection. As to the remaining drag contributors, he remarks that the estimation of their drags “is largely a matter of intelligent guesswork assisted by a woefully small amount of data derived from tunnel and flight tests.” He adds that “External fittings and excrescences are allowed for by finding a tunnel test on something resembling the item in question and applying a similar drag coefficient”. The implications for further penetration into ‘the jet age’ are clear: more advanced theoretical methods combined with extensive wind tunnel and flight tests will be crucial to further progress.

It seems appropriate to end this survey with that most sleekly elegant of early British swept-wing aircraft, the Hawker Hunter. Results for a 1/5 scale model of it tested in the RAE’s 11.5 ft tunnel are contained in a report, dated June 1950, by Kirby and Holford⁽⁴⁴⁾. The tunnel speed was 120 ft/s and the test Reynolds number 1.6×10^6 based on the wing mean chord. The model was fitted with a duct from the intakes to the tailpipe which was throttled to give something like the airflow required for the engine. Although the report’s main concern centres on stability issues, test results provide C_D data over a range of C_L values. Brinkworth⁽⁴⁵⁾ has analysed these data and reports a C_{D0} value of 0.0139. In this he has used the procedure described above in which a graph of C_D against C_L^2 is plotted. The graph’s line here is gratifyingly straight, there being no Re variation involved in this case. Extrapolation to $C_L = 0$ then yields the above estimate for C_{D0} . The graph’s gradient is 0.122 so that, the aspect ratio A being 3.24, the value for k is 1.24. It would be interesting to compare the C_{D0} estimate with the value obtained from flight tests of the full-scale aircraft for which the Reynolds number would be more than twenty times higher than that of the tunnel tests.

7. Concluding Remarks

The survey has attempted to set down the main steps needed to both understand the origins of drag and reduce its adverse effects on aircraft performance. Having provided a large number of examples, it is hoped that this survey might prove useful in the ongoing debate concerning performance comparisons of famous aircraft.

It is felt that, for the British, it was Jones⁽¹⁸⁾ in 1929 who provided the much-needed impetus for improvement. Lest it be thought that this came rather late in the day, it should be remembered that the necessary wherewithal for this, the new boundary-layer and wing theories, had only begun to penetrate Britain’s scientific and technical consciousness a mere six or seven years earlier.

Jones’s plan for improvement was to pare away parasite drag to such an extent that the only drag remaining was that which could not be eradicated, the drag due to the boundary layer. However, later application of his method, based on flat plate turbulent boundary layer data, led to underestimation of this drag contribution and improvement in this respect did not occur until RAE staff provided more accurate methods^(29, 30) in the late 1930s. Meanwhile, attempts such as that by Morgan⁽²⁵⁾ at the RAE to pin down the various parasite drag contributions, hampered as this was by boundary-layer drag underestimation on the one hand

and rather inaccurate parasite drag prediction on the other, nonetheless showed the way forward. In this respect, a further problem concerned the accuracy with which total drag was predicted from flight-test data. Total drag being equal to total engine thrust in steady level flight, it was necessary to improve the accuracy with which propeller efficiency was calculated and to take correct account of the thrust augmentation effects provided by ejector exhausts and ducted radiators. Again, the RAE made considerable progress in these areas. Around 1940 all of these advances were shown to advantage in the drag assessments made by Collar⁽²⁴⁾ and, more particularly, by Hufton⁽³³⁾ at the RAE for relatively well-streamlined fighter aircraft. And at that time Bottle⁽³⁶⁾ showed that this method worked almost equally well when applied to necessarily more parasite drag prone bombers. These advances in drag assessment then successfully carried over to the early jet age, as Courtney⁽⁴³⁾ demonstrated in 1950. During much of this period, whilst the RAE was engaged in developing more specialist advances in aerodynamics, its staff were also occupied with the bread-and-butter activity of compiling an extensive data base⁽³⁹⁾ detailing the core aerodynamic features of a wide range of aircraft. This has proved extremely useful here in tracing the 'history of C_{D0} '.

To reach this far in this 'history' has taxed the stamina of this old C_{D0} geek, and doubtless the reader's patience. Nonetheless, it would be interesting to bring the story closer to the present day, not least because this would produce a far greater tribute to the RAE than that of this paper. It was one thing for the RAE to deal with the aerodynamic exigencies of the wartime period and its immediate aftermath of the early jet age but expertise of a greater order of magnitude was needed to devise the aerodynamic advances for Concorde and the Airbus wing design. To cover these major challenges faced by staff at both Farnborough and the newly-founded Bedford site, however, would be no mean feat since it would depend heavily on tracing such data as remain from wilfully abandoned government laboratories and now-defunct manufacturers. Perhaps another writer might take up such a considerable challenge?

Acknowledgements

The author gratefully acknowledges the generous assistance of Brian Riddle, Librarian of the Royal Aeronautical Society, and Anthony Pilmer of the National Aerospace Library, Farnborough. Gratitude must also be expressed to the late Harry Fraser-Mitchell FRAeS and Frank Armstrong FREng FRAeS for alerting the author to the RAE C_{D0} database's existence, to Geoffrey Butler FRAeS (Farnborough Air Sciences Trust (FAST)) for providing copies of such documents, to Professor Brian Brinkworth FREng, FRAeS and Michael Marsden for further data, to Professor Gareth Padfield FREng, FRAeS for data relating to the Wright Flyers, to Dr-Ing Johannes Traugott (Technischen Universität München) for data on the albatross, and to Dr Christopher Mitchell FRAeS and Evolve Design Consultants for assistance with some of the graphics.

References

1. ACKROYD, J. A. D. Babinsky's Demonstration: The Theory of Flight and Its Historical Background. *J. Aero. Hist.*, 2015, **5**, pp 1-42. <https://www.aerosociety.com/publications/jah-babinsky-s-demonstration-the-theory-of-flight-and-its-historical-background/>
2. ACKROYD, J. A. D. The aerodynamics of the Spitfire. *J. Aero. Hist.*, 2016, **6**, pp 59-86. <https://www.aerosociety.com/publications/jah-the-aerodynamics-of-the-spitfire/>
3. FINSTERWALDER, S. Die Aerodynamik als Grundlage der Luftschiffahrt Vortrag. *Zeitschrift für Flugtechnik und Motorluftschiffahrt*, 1910, **1**, pp 6-10, 30-31.
4. LILIENTHAL, O. *Der Vogelflug als Grundlage der Fliegekunst*. Gaertners, Berlin, 1889. [*Birdflight as the Basis of Aviation*. Trans. Isenthal, A. W., Longmans Green & Co., London, 1911.]
5. LOFTIN, L. *Quest for performance. The evolution of modern aircraft*, NASA SP 468, NASA, Washington DC, 1985. <https://history.nasa.gov/SP-468/contents.htm>
6. NEWTON, I. *Philosophiae Naturalis Principia Mathematica*. London, 1687. [*Mathematical Principles of Natural Philosophy*. Trans. Third Latin Edition by MOTTE, A, London, 1729.]
7. GIBBS-SMITH, C. H. *Sir George Cayley's Aeronautics 1796-1855*. HMSO, London, 1962.
8. CAYLEY, G. On aerial navigation, *A Journal of Natural Philosophy, Chemistry and the Arts*, 1809, **24**, pp 164-174; 1810, **25**, pp 81-87, 161-169.
9. LANGLEY, S. P. *Experiments in Aerodynamics*. Smithsonian Institution, Washington DC, 1891.
10. PRANDTL, L. Über Flüssigkeitsbewegung bei sehr kleiner Reibung. *Verhandlungen des dritten internationalen Mathematiker-Kongresses in Heidelberg, 8-13 August 1904*. pp 489-491, Teubner, Leipzig, 1905.
11. BLASIUS, P. R. H. Grenzschichten in Flüssigkeiten mit kleiner Reibung. *Zeit. für Mathematik und Physik*, 1908, **56**, pp 1-37.
12. PRANDTL, L. Tragflügeltheorie, I *Mitteilungen. Nach der kgl Gesellschaft der Wiss zu Göttingen, Math-Phys Klasse*, 1918, pp 451-477.
13. PRANDTL, L. Tragflügeltheorie, II *Mitteilungen. Nach der kgl Gesellschaft der Wiss zu Göttingen, Math-Phys Klasse*, 1919, pp 107-137.
14. GLAUERT, H. *Aerofoil and Airscrew Theory*. Cambridge University Press, 1926.
15. PADFIELD, G. D. and LAWRENCE, B. The birth of the practical aeroplane: An appraisal of the Wright brothers' achievements in 1905. *Aeronaut J*, 2005, **109**, pp 421- 437.
16. LAWRENCE, B. The Flying Qualities of the Wright Flyers, PhD thesis, September 2004, Dept of Engineering, University of Liverpool, UK. A paper based on the thesis is available at <http://pcwww.liv.ac.uk/eweb/fst/publications/Wright1905.pdf>
17. ANDERSON, J. D. *The Airplane. A History of Its Technology*. AIAA. Reston VA, 2002.
18. JONES, B. M. The streamline aeroplane. *JRAeS*, 1929, **33**, pp 357-385.

19. PRANDTL, L. Über den Reibungswiderstand strömender Luft. *Ergebnisse der Aerodynamischen Versuchsanstalt zu Göttingen*, 1927, **3**, pp 3-5.
20. HELE-SHAW, H. S. and BEACHAM, T. E. The variable pitch airscrew. *JRAeS*, 1928, **32**, pp 525–554.
21. SACHS, G. Minimum shear wind strength required for dynamic soaring of albatrosses. *Ibis*, 2005, **147**, pp 1-10.
22. AERODYNAMIC STAFF, RAE. Some aerodynamic figures of merit. RAE Report No. BA 1275 (Rewritten), January 1937.
23. AERODYNAMIC STAFF, RAE. Notes on aerodynamic criteria for some recent service aeroplanes. RAE Report No. BA 1430, October 1937.
24. COLLAR, A. R. The performance of the ‘Hurricane’ and ‘Spitfire’ aeroplanes. ARC, Ae 1674, June 1940.
25. MORGAN, M. B. Note on drag analysis of various types of aeroplane. RAE Report No. BA 1499, August 1938.
26. MEREDITH, F. W. Note on the cooling of aircraft engines with special reference to ethylene glycol radiators enclosed in ducts. ARC, R & M No. 1683, 1935.
<http://naca.central.cranfield.ac.uk/reports/arc/rm/1683.pdf>
27. CAPON, R. S. The cowling of cooling systems. ARC, R & M No. 1702, 1936.
28. HARTSHORN, A. S., DIPROSE, K. V. & PATTERSON, G. N. On the thrust obtainable from exhaust momentum. RAE Report No. BA 1578. March 1940.
29. SQUIRE, H. B. and YOUNG, A. D. The calculation of the profile drag of aerofoils. ARC, R & M No. 1838, 1937. <http://naca.central.cranfield.ac.uk/reports/arc/rm/1838.pdf>
30. YOUNG, A. D. The calculation of the total and skin friction drags of bodies of revolution at zero incidence. ARC, R & M No. 1874, 1939.
<http://naca.central.cranfield.ac.uk/reports/arc/rm/1874.pdf>
31. RELF, E. F. Recent research on the improvement of the aerodynamic characteristics of aircraft. *JRAeS*, 1938, **42**, pp 512-535.
32. YOUNG, A. D. *Boundary Layers*. BSP Professional Books, Oxford, 1989.
33. HUFTON, P. A. An analysis of the performance of the high speed Spitfire and a standard Spitfire. RAE B. A. Departmental Note – Performance No. 12, April 1940.
34. MORGAN, E. B. and SHACKLADY, E. *Spitfire: The History*. Key Publishing, Stamford, Lincs, 1987.
35. BRINKWORTH, B. J. Spitfire ‘Tailplane Protection’ and spinning trials. *J. Aero. Hist.*, 2017, **7**, pp 16-24. <https://www.aerosociety.com/publications/jah-spitfire-tailplane-protection-and-spinning-trials/>
36. BOTTLE, D. W. Analysis of the drag of a number of bombers at top speed. RAE B. A. Departmental Note – Performance No. 24, November 1940.
37. COOPER, H. J. and THETFORD, O. G. *Aircraft of the Fighting Powers, Vol. 1*. Harborough, Leicester, 1941.

38. GREEN, W. *Warplanes of the Third Reich*. MacDonald, London, 1970.
39. RAE STAFF. Structural weight and drag analyses for British and American aircraft. RAE Tech. Note SME 96, Aero 1092. Issue 1 c1942 (Addendum January 1943), Issue 2 November 1943, Issue 3 August 1945 (Addenda October 1945, April 1946).
40. MAIR, W. A. (Ed). Research on high speed aerodynamics at the Royal Aircraft Establishment from 1942 to 1945. ARC, R & M No. 2222, 1950.
41. BINKWORTH, B. J. On the aerodynamics of the Gloster E28/39 - a historical perspective. *Aeronaut. J.*, 2008, **112**, (1131), pp 307–326.
42. AERODYNAMIC STAFF, RAE. Drag analysis of the Canberra and brief comparison with flight tests. RAE Technical Memorandum No. Aero. 142, December 1950.
43. COURTNEY, A. L. Profile drag analysis of Supermarine E. 41/46, Hawker E. 38/46 and North American F. 86A, with notes on method of drag estimation. RAE Tech. Note Aero. 2074, December 1950.
44. KIRBY, D. A. and HOLFORD, J. F. Low speed tunnel tests on a 1/5th scale model of a single-jet fighter with a 40° sweptback wing (Hawker F.3/48). RAE Report Aero 2382, June 1950.
45. BRINKWORTH, B. J. Letter to the author. August 2017.
46. CAYLEY, G. Sir George Cayley's Governable Parachutes, *Mechanics' Magazine*, 1852, **57**, pp 241-244.
47. ANDERSON, J. D. *Introduction to Flight, Its Engineering and History*. McGraw-Hill, New York, 1978.
48. KUTTA, M. W. Auftriebskräfte in strömenden Flüssigkeiten. *Illus. Aeronautische Mitteilungen*, 1902, **6**, pp 133-135.
49. ZHUKOVSKII, N. E. Über die Konturen der Tragflächen der Drachenflieger. *Zeitschrift für Flugtechnik und Motorluftschiffahrt*, 1910, **1**, pp 281-284.
50. ACKROYD, J. A. D. Lanchester – The Man (The 31st Lanchester Lecture). *Aeronaut. J.*, 1992, **96**, (954), pp 119-140.
51. LANCHESTER, F. W. *Aerodynamics*. Constable & Co Ltd, London, 1907.
52. BAZZOCCHI, E. Technical aspects of the Schneider Trophy and the world speed record for seaplanes. *Aeronaut. J.*, 1972, **76**, (734), pp 65-82.
53. ANDREWS, C. F. and MORGAN, E. B. *Supermarine Aircraft since 1914*. Putnam, London, 1981.
54. JAMES, D. N. *Schneider Trophy Aircraft 1913 – 1931*. Putnam, London, 1981.
55. ANDREWS, C. F. and COX, W. G. The Supermarine S4 – S6B. *Aircraft in Profile, Vol. 2*, Profile Publications Ltd., Windsor, Berks. 1965.
56. HEINKEL, E. Schnellpostflugzeug He 70. *Zeitschrift für Flugtechnik und Motorluftschiffahrt*, 1933, **24**, (24), pp 669-676. [The high-speed Heinkel He 70 mail airplane. NACA Tech. Memo. No. 746, 1934.]

57. JONES, R. and SMYTH, E. Experiments on a Heinkel He. 70 aeroplane in the Compressed Air Tunnel. ARC, R & M No. 1709, 1936.
58. HUFTON, P. A. and SMITH, A. G. Short performance tests on Heinkel He 70 with Rolls Royce Kestrel XVI (V. P.). RAE Report No. BA 1364. January 1937.
59. HUFTON, P. A. Preliminary note on the cleanness efficiency of the Heinkel He 70. RAE Report No. BA 1401. May 1937.
60. SHAW, R. A. and DIPROSE, B. A. Tests on the Heinkel He 70 in the 24 ft. tunnel. RAE Report No. BA 1445. December 1937.
61. CAMBRIDGE UNIVERSITY AERONAUTICAL LABORATORY. The measurement of profile drag by the pitot-traverse method. ARC, R & M No. 1688, 1936.
62. HUFTON, P. A. An analysis of some performance tests on the Heinkel He 70 with Rolls Royce Kestrel XVI. RAE Report No. BA 1474. May 1938.

Appendix 1

The Importance of L/D Ratio and Its Maximum Value

In his Notebook entry for 1st December 1804 Cayley states ⁽⁷⁾ that his first glider, the world's first aeroplane, descended steadily at a speed of 15 ft/s in still air conditions and at an angle of 18° below the horizontal. The situation for any such glider is shown in Figure 11, the gliding angle here being γ . The glider's weight is W and, using the triangle of forces shown, it is seen that the weight component along the glide path and in the direction of steady motion is $W \sin \gamma$. The weight component perpendicular to this motion is $W \cos \gamma$. Thus $W \sin \gamma$ provides the propulsive thrust for this motion so the glider's drag force, D , which precisely opposes this is given by

$$D = W \sin \gamma.$$

The lift force, L , by definition, is perpendicular to the direction of motion so that

$$L = W \cos \gamma.$$

Consequently, the lift-to-drag ratio, L/D , is

$$L/D = \cos \gamma / \sin \gamma = 1 / \tan \gamma. \quad (\text{A1.1})$$

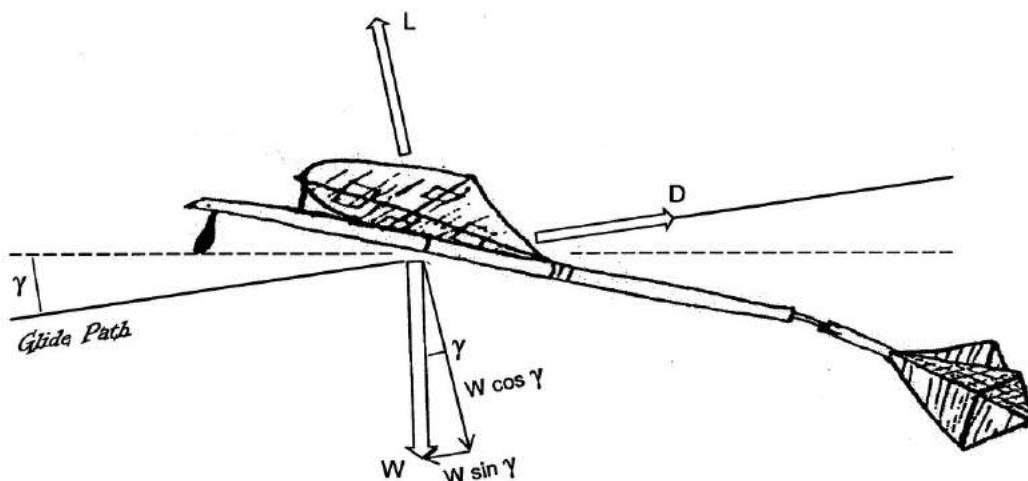


Figure 11 Gliding flight in still air conditions

Clearly it is advantageous to achieve the smallest possible gliding angle and, by equation (A1.1), this requires the L/D ratio to be as high as possible. Cayley's gliding angle, $\gamma = 18^\circ$, indicates an L/D ratio around 3. For his 'Governable Parachute' of 1852 Cayley ⁽⁴⁶⁾, in contrast, suggested that this glider would travel a horizontal distance 5 to 6 times its release height, implying an L/D ratio between 5 and 6.

A further indicator of the importance of the L/D ratio is provided by a theoretical analysis to determine the distance flown by a propeller-driven aeroplane until its fuel is completely exhausted. The analysis is rather lengthy and can be found in a number of standard texts on aeronautics, for example Reference 47. The situation envisaged in the analysis is rather simplistic in the sense that no climb-out and descent-to-landing are included and the aeroplane is assumed to fly throughout at a fixed value of the L/D ratio. The result for the distance flown, known as the Breguet range relation, reveals that this distance is directly

proportional to the L/D ratio. Consequently improvement of that ratio provides a proportionate improvement in range.

In order to determine an aeroplane's maximum L/D ratio it is advantageous to put the problem a slightly different way: under what circumstances is the D/L ratio a minimum? This makes the mathematical analysis rather more straightforward. According to equations (5) and (6),

$$C_D = C_{D0} + BC_L^2, \text{ where } B = k/(\pi A).$$

Since Drag, $D = \frac{1}{2}\rho V^2 SC_D$ and Lift, $L = \frac{1}{2}\rho V^2 SC_L$, then

$$D/L = C_D / C_L = C_{D0}/C_L + BC_L^2 / C_L = C_{D0}/C_L + BC_L.$$

The only variable on the right hand side of this relation is C_L . Using differential calculus, the rate of change of D/L with respect to variation in C_L is

$$d(D/L)/dC_L = -C_{D0}/C_L^2 + B.$$

This is a maximum, a minimum or a point of inflexion when $d(D/L)/dC_L = 0$, ie $C_L^2 = C_{D0}/B$ or when $C_{D0} = BC_L^2$, the induced drag coefficient then being equal to C_{D0} . The calculation of $d^2(D/L)/dC_L^2$ at this value of C_L reveals that the case of interest is a minimum. Therefore,

$$(D/L)_{\min} = C_{D0}/(C_{D0}/B)^{1/2} + B(C_{D0}/B)^{1/2} = (BC_{D0})^{1/2} + (BC_{D0})^{1/2} = 2(BC_{D0})^{1/2}.$$

Thus, $(L/D)_{\max} = \frac{1}{2}(\pi A/(kC_{D0}))^{1/2}$. (A1.2)

This maximum value is seen in Figure 2 of the main text. One further feature of that figure worth discussing is the slope of the $C_L \sim$ incidence graph, the incidence angle being α . Prandtl⁽¹²⁾ showed that this slope depends on wing aspect ratio, A, the result for the elliptic loading case ($k = 1$) given by Glauert⁽¹⁴⁾ being

$$dC_L/d\alpha = 2\pi A / (2 + A). \quad (A1.3)$$

As the aspect ratio A tends to infinity, the slope thus correctly increases to the limit of 2π which is the result given by the aerofoil theories of Kutta⁽⁴⁸⁾ in 1902 and Zhukovskii⁽⁴⁹⁾ in 1910. This variation of the slope with aspect ratio springing from Prandtl's work is shown in Figure 12 taken from Reference 50. Included in the figure is the graph of the results obtained by Lanchester⁽⁵¹⁾ in 1907. As Reference 50 shows, Lanchester's result is

$$dC_L/d\alpha = 2\kappa(\epsilon + 1),$$

where κ and ϵ are empirical variables of dubious provenance for which Lanchester⁽⁵¹⁾ is nonetheless able to estimate their values over a range of aspect ratios. Although Lanchester's results shown in Figure 12 underestimate Prandtl's correct variation, they nonetheless show a similar trend. Lanchester⁽⁵¹⁾ also predicted the variation of induced drag, giving the result

$$C_{Di} = C_L^2 / [4\kappa(1 + \epsilon) / (1 - \epsilon)].$$

Prandtl's equivalent result for the elliptic loading case $k = 1$ is (equation (5))

$$C_{Di} = C_L^2 / (\pi A).$$

The two results differ only in the form of their denominators and Figure 13, taken from Reference 50, shows their variations with aspect ratio. Lanchester's result for induced drag is thus seen to be close to that of Prandtl.

As is well-known, Lanchester's work of 1907 in aerodynamics⁽⁵¹⁾ was largely ignored in Britain, despite his membership of the Advisory Committee for Aeronautics since its foundation in 1909. Thus his rather rudimentary concept of the boundary layer, which he called the inert layer, and his semi-empirical circulation theory for wing lift had no impact on aeronautical research in Britain. Moreover, the British aeronautical community remained entirely innocent of the major and more rigorous

advances abroad: Prandtl's boundary-layer theory⁽¹⁰⁾, the circulation theories of Kutta⁽⁴⁸⁾ and Zhukovskii⁽⁴⁹⁾ for aerofoils and their extension by Prandtl^(12, 13) to wings. Thus British work in aerodynamics remained largely an experimental activity. For example, the various aerofoil section shapes devised, often by cut-and-try methods, were usually tested on wings of aspect ratio six, the results being displayed graphically in forms similar to Figure 2. Thus there was no realisation that the slopes of the $C_L \sim \alpha$ graphs were, by equation (A1.3), close to three-quarters of 2π and that this could be improved by use of higher aspect ratios.

Similarly there was no understanding that the rise of C_D with α was due to induced drag and that this too could be improved by choice of higher aspect ratio. The situation changed rapidly, however, once Glauert had visited Göttingen after the close of the First World War. Thereafter, as described in Reference 1, British research in aerodynamics advanced rapidly during the 1920s. What then became required, as evidenced by Jones's plea⁽¹⁸⁾ of 1929, was that designers should put it into common practice. As the 1930s advanced some, at least, realised that the world had begun to drift into uncertain times. The doctrine at that time, it will be recalled, was that the bomber would always get through and the fear was that this might translate into an all-too-terrifying reality. Thus the 300 mph more heavily-armed fighter with a high rate of climb would be crucial in countering this.

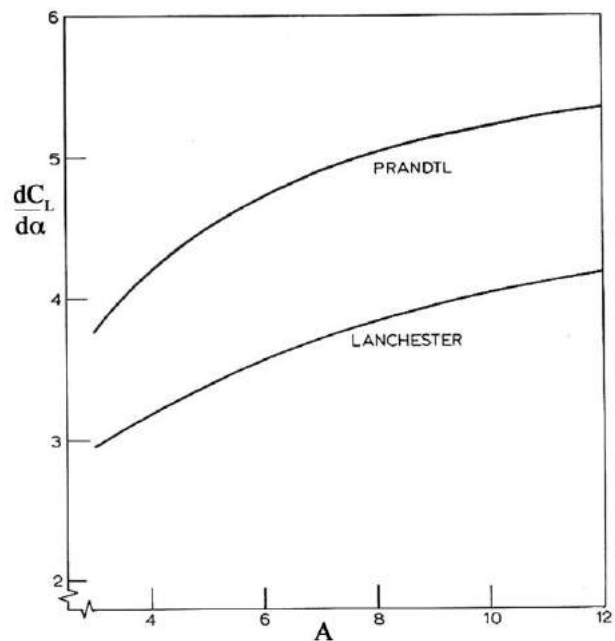


Figure 12 Variation of lift curve slope with aspect ratio

Source: Ackroyd, Reference 50

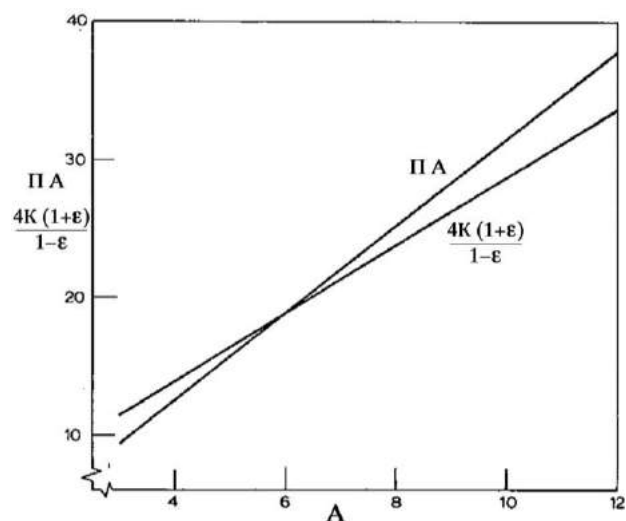


Figure 13 Variation of induced drag factor with aspect ratio Source: Ackroyd, Reference 50

Appendix 2

The Aeroplane's Power & Lift Requirements

For an aeroplane in steady level flight at constant speed the total propulsive thrust, T , must precisely oppose the drag, D . The power required to sustain this motion is TV . For an aeroplane solely dependent on an engine-propeller combination for its propulsion, the engine power being P and propeller efficiency η , the power provided by the propeller is ηP . Thus,

$$\eta P = TV = DV = \frac{1}{2} \rho V^3 S C_D \quad (\text{A2.1})$$

or
$$V^3 = 2\eta P / (\rho S C_D). \quad (\text{A2.2})$$

Essentially this is the result stated by Loftin⁽⁵⁾ which he uses as the basis for his assessment of aeroplane performance.

To see how this V^3 relationship affects the speed performance of an aeroplane, consider the case of the first powered aeroplane to achieve sustained, controllable flight, the Wright Flyer 1 of 1903. Its extensively braced biplane assembly produced a very high value of C_D . This and its low value of P resulted in a maximum value for V of around 30 mph. With no other changes being made, suppose that P could be boosted by a factor of 100. In that case, according to equation (A2.2), V^3 would be equally enhanced and V itself increased by the cube root of 100, which is roughly 4.6. Thus the speed would become a little short of 140 mph, a worthwhile speed enhancement but at the expense of an enormous power increase. To put the latter to better use, suppose that by careful streamlining C_D could be reduced to one fifth of its previous value and sufficient lift could be obtained by a single wing, a monoplane, of an area one half that of the Flyer. This combination of aerodynamic improvements, $1/5$ and $1/2$, or a reduction to $1/10$ of the product $C_D S$, gives a further boost of 10 to our original power-produced boost of 100. This yields a total boost to V^3 of not the earlier 100 but 1,000. The latter's cube root is 10 so the original top speed of 30 mph is multiplied by this factor to yield a speed of around 300 mph. In contrast, if no aerodynamic improvements had been employed then the reduction of $1/10$ in the product $C_D S$ would have to have been replaced by a power increase factor of 1,000. Given that the Flyer 1's power was around 10 hp, an aeroplane, however configured but possessing the Flyer's high $C_D S$ value, would have required an engine power of about 10,000 hp in order to achieve a speed of around 300 mph.

But how might the above improvement in top speed affect the aeroplane's performance at low speed, in particular the pilot's ability to handle the aircraft at that condition? According to equation (4), the relation for the lift force, L , is

$$L = \frac{1}{2} \rho V^2 S C_L, \quad (\text{A2.3})$$

C_L being the lift coefficient which depends predominantly on a wing's incidence angle (see Figure 2).

In steady level flight at constant speed, the lift must precisely oppose the aeroplane's weight, W :

$$L = W.$$

By equation (A2.3),

$$V^2 = 2w/(\rho C_L), \quad (\text{A2.4})$$

where

$$w = W/S$$

is the wing loading. To return to the examples chosen for the power ~ speed comparison above, again suppose that a wing area half that of the Wright Flyer 1 is selected. Furthermore, suppose that, with its much more powerful but heavier engine and a metal structure of much greater weight, this monoplane's total weight has increased, say, by a factor of eight. Consequently, wing loading w has increased by a factor of sixteen. If there are no changes to air density and the maximum value of C_L available, according to equation (A2.4), V^2 must also increase by this same factor. The lowest value of V would then increase by a factor equal to the square root of sixteen, which is four. Whereas the Flyer 1 might have sustained itself in flight at a little over 20 mph, this much heavier monoplane's lowest speed would be of the order of 80 mph. In order to make this monoplane more manageable for the pilot at the low speeds of take-off or landing, an increase in C_L through the use of trailing edge flaps/leading edge slats might bring this speed down to a more acceptable 60 mph value.

The above exercises are far from hypothetical. The Flyer 1 of 1903 has a wing area of 510 ft² and weighs 745 lbs. It is powered by an engine of 12 hp which, taking the propeller efficiency η to be about 0.67, yields a power at the propeller around 8 hp. These data can be compared with those of the early marks of the Spitfire, for which engine power is a little over 1000 hp. The propeller efficiency η is 0.80 so that power at the propeller is slightly above 800 hp, roughly one hundred times that of the Flyer. The Spitfire's wing area is 242 ft², a little less than half that of the Flyer, whereas its weight is 5820 lbs. Thus its wing loading, w , is slightly more than sixteen times higher than that of the Flyer 1. As to the crucial factor of drag, modern assessments of the Flyer suggest that at its highest speed it flew at a C_D value around 0.1. In contrast, having benefitted from a high degree of streamlining, the Spitfire and its contemporaries such as the Hurricane and Bf 109 achieved C_D values around 0.02, roughly one fifth that of the Flyer. In fact, due to its C_D value being the lowest of those above, together with thrust assistance from its engine exhaust and radiator hot air ejection (see below), the Spitfire achieved a maximum speed around 360 mph, significantly higher than our 300 mph rough estimate. However, as a further illustration of the $P \sim V^3$ relation (A2.2), it is worth noting that during its impressive development the Spitfire's engine power roughly doubled. On that basis its maximum speed would be expected to increase by a factor of roughly the cube root of two, which is about 1.26. This suggests a maximum speed around 450 mph, close to that actually achieved by the final Spitfire marks.

As noted above, the Spitfire and its contemporaries designed in the mid-1930s benefitted from additional thrust, T_j , provided by rearward ejecting engine exhausts and heat regeneration in their ducted radiators. The power enhancement provided by these devices is then $T_j V$. Consequently equation (A2.1) now takes the form

$$\eta P + T_j V = DV = \frac{1}{2} \rho V^3 S C_D. \quad (\text{A2.5})$$

The important point here is that a calculation of C_D based solely on the power at the propeller term ηP , the approach taken by Loftin⁽⁵⁾, will result in an underestimation of C_D .

In the late 1920s and throughout the period of the Second World War it became common practice in Britain to scale drag results from wind tunnel and flight tests to the drag experienced at sea level and at a speed of 100 ft/s. This made it easier to compare drag results of one aircraft with another and with results obtained in the RAE's 24 ft Open Jet Tunnel. The analysis required to achieve this scaling has been given in Appendix 1 of Reference 2 but is repeated here for ease of reference. It follows from equation (A2.5) that

$$\eta P / (V^3) + T_j / (V^2) = \frac{1}{2} \rho S C_D.$$

Writing $\sigma = \rho/\rho_0$, ρ_0 being the sea-level air density, then

$$\eta P / (\sigma V^3) + T_j / (\sigma V^2) = \frac{1}{2} \rho_0 S C_D.$$

However,

$$\frac{1}{2} \rho_0 S C_D (100)^2 = D_{100} \quad (\text{A2.6})$$

is the drag at sea level at a speed of 100 ft/s. Consequently,

$$10^4 \eta P / (\sigma V^3) + T_{j,100} = D_{100} \quad (\text{A2.7})$$

$$T_{j,100} = 10^4 T_j / (\sigma V^2), \quad (\text{A2.8})$$

the latter being the exhaust/radiator thrust at a speed of 100 ft/s. The term

$$10^4 \eta P / (\sigma V^3) = T_{e,100} \quad (\text{A2.9})$$

is then the engine/propeller thrust at 100 ft/s.

In flight-test work with aeroplanes propelled by a piston engine the values of η , P and T_j , if appropriate, must be known with certainty at the altitude at which the speed, V , has been measured. With that information, C_D can be calculated from the above relations. However, for an aeroplane propelled solely by a jet engine it is the thrust T_j which is known. In this case the basic relationship (A2.1) becomes

$$T_j = D = \frac{1}{2} \rho V^2 S C_D. \quad (\text{A2.10})$$

When scaled to sea level conditions and a speed of 100 ft/s, the expression for $T_{j,100}$ is then that given by equation (A2.8).

Appendix 3

The Value of C_{D0} for Jones's 'Streamline Aeroplane'

In order to estimate the boundary-layer drag on aeroplanes, Jones⁽¹⁸⁾ bases his calculations on known skin-friction relations for flat plates experiencing laminar or turbulent boundary-layer flows. Since these flows are due entirely to the action of the air's viscosity, the latter's influence enters results in terms of the Reynolds number

$$Re = \rho V \ell / \mu,$$

where ℓ is the streamwise length of the body and μ is the viscosity coefficient. The skin friction relations are shown in Figure 14 taken from Jones's paper⁽¹⁸⁾ in which he plots the skin friction coefficient k_F against Reynolds number Re . This coefficient he defines as

$$k_F = (\text{skin friction drag}) / (\rho V^2 E), \tag{A3.1}$$

E being the *total* wetted surface area of the plate which is *twice* S , its planform area. This, together with the lack of the factor of $\frac{1}{2}$ in the definition of k_F , gives $k_F = C_D/4$. For laminar boundary layers he quotes the result given by Blasius⁽¹¹⁾ (equation (3)) and confirmed by experiment,

$$k_F = 0.66 Re^{-1/2}. \tag{A3.2}$$

For turbulent boundary layers he turns to Prandtl's result⁽¹⁹⁾ drawn from a survey of experimental data (equation (8)):

$$k_F = 0.019 Re^{-0.15}. \tag{A3.3}$$

COMPARISON BETWEEN PROFILE DRAG OF WELL-KNOWN WINGS AND THE SKIN-FRICTION ON A FLAT PLATE.

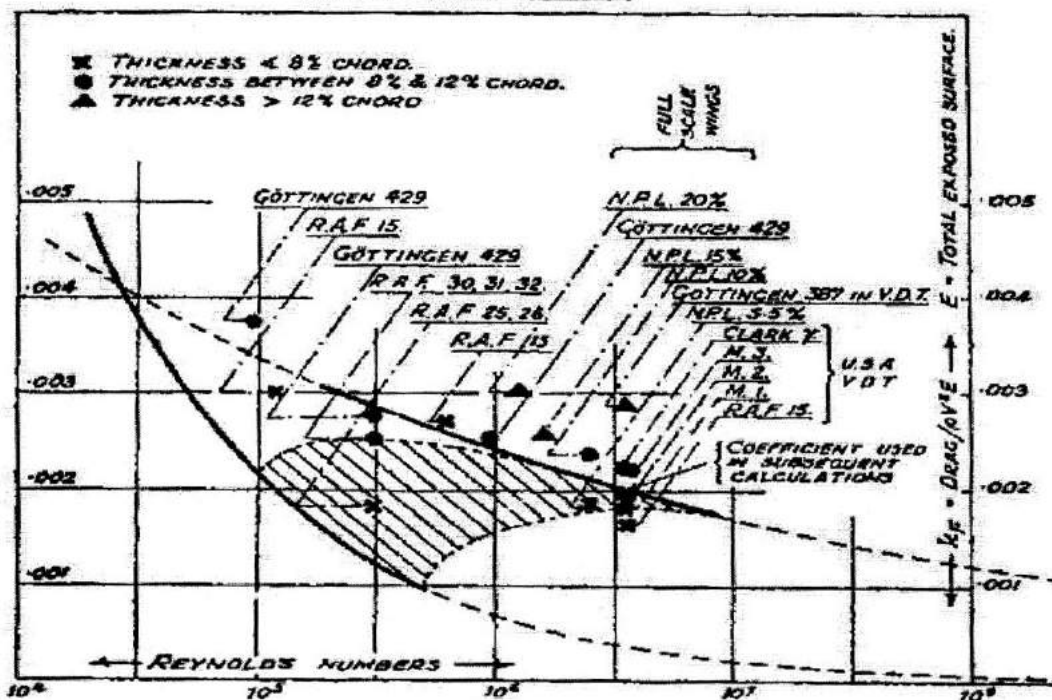


Figure 14 Variation of drag for plates and aerofoils with Reynolds Number
Source: Jones, Reference 18

Jones⁽¹⁸⁾ points out that, in practice, departure from the lower, laminar curve of Figure 14 can occur when turbulent transition begins, the curve looping upward to join the upper turbulent curve. Although the process of transition was not understood at the time, it was known that this often, but not always, tended to occur in the Re range 10^5 and 5×10^5 ; hence the shaded area in the figure indicating the possible transition region. Included in Figure 14 are results for a variety of current aerofoil sections, most of which lie on or slightly above the turbulent curve. He argues that, due to the high Reynolds numbers achieved in full-scale flight, the skin friction drag on aeroplane wings will lie close to the turbulent curve. He then turns to bodies of revolution, citing a number of experimental results obtained from a series of airship shapes. The wetted area for these shapes he takes to be three-quarters the area of their circumscribing cylinders. The results, when displayed in this form in Figure 15, are strikingly similar to those for flat plates in Figure 14.

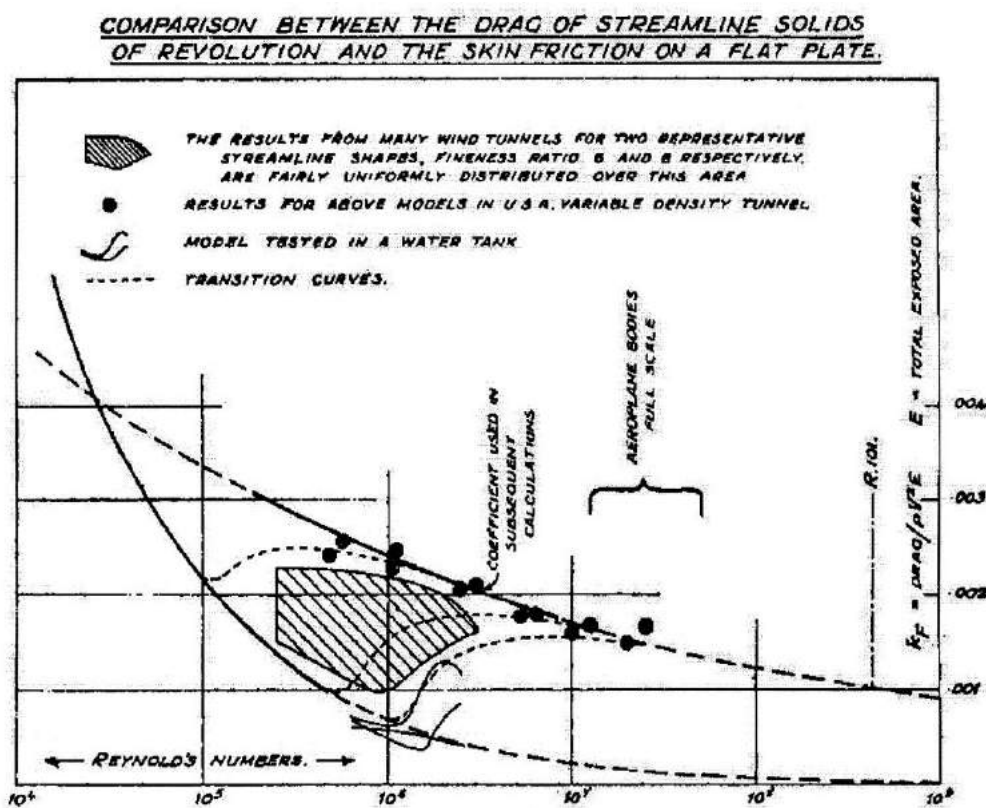


Figure 15 Variation of drag for axisymmetric bodies with Reynolds Number

Source: Jones, Reference 18

For the estimation of aeroplane drag due to its boundary layer, Jones⁽¹⁸⁾ explains that, having selected a Reynolds number representative of full-scale flight, the corresponding value for k_F can be obtained from equation (A3.3). He points out that, for full-scale aeroplanes at full speed, the Re values based on wing chord as the length scale vary between 4×10^6 and 10^7 , the corresponding values of k_F ranging from 0.0020 to 0.0017. In contrast, representative Re values based on fuselage length lie between 2×10^7 and 5×10^7 , the corresponding k_F values varying from 0.00155 to 0.00135. “So as to leave a little in hand”, as Jones⁽¹⁸⁾ puts it, he selects a k_F value of 0.0020 for his streamline aeroplane. He is then left with the problem of selecting a value for E , the aeroplane’s total wetted area. Having surveyed a number of

current aircraft, he finds that the ratio E/S (S being the wing planform area) varies between 3.0 and 3.5. Taking $E/S = 3.2$ as an average value and using equation (A3.1), his result for the streamline aeroplane's boundary-layer drag at zero lift, D_0 , is

$$D_0 = 0.0020 \rho V^2 E = 0.0020 \times 3.2 \rho V^2 S = 0.0040 \times 3.2 (1/2 \rho V^2 S).$$

Although Jones does not take this step, when recast in terms of C_{D0} his result yields

$$C_{D0} = D_0 / (1/2 \rho V^2 S) = 0.0128.$$

Had he chosen the k_F value of 0.0035 for the highest Reynolds number of 5×10^7 , his value for C_{D0} would have been 0.0086. This is close to the values used later at the RAE as described in Section 5.

Jones⁽¹⁸⁾ raises two further points of interest here. The first is that in Figure 14 the drags of aerofoils of small thickness-chord ratio tend to lie slightly below the turbulent curve whereas thicker aerofoils, particularly those marked by black triangles (\blacktriangle) with thickness-chord ratios between 12.5% and 20%, lie significantly above the curve. Subsequent wind-tunnel studies in Britain in the mid-1930s seemed initially to contradict this. As described in Section 3 of Reference 2, this led to some confusion when it came to the choice of wing thickness-chord ratio for certain fighter aircraft. Luckily the matter was resolved within a couple of years and Jones's prognostication was proved correct.

The second point raised in Jones's lecture concerns some of the experimental data shown in Figure 15. Jones⁽¹⁸⁾ argued, correctly as it turned out, that the point at which transition to turbulence occurred seemed to depend on the turbulence level of the wind tunnels used. Those with lower turbulence levels appeared to produce later onsets of turbulence than those having high turbulence levels. Jones⁽¹⁸⁾ then drew attention to the two experimental curves shown as elongated S-shaped lines at Reynolds numbers slightly above 10^6 . These results, he explained, had been obtained in the naval tank of the National Physical Laboratory. In this case the airship models had been pushed steadily through water at rest, the results suggesting that when the turbulence level is extremely low a delay in the onset of transition appeared possible. This offered the possibility of extending the laminar boundary-layer region and thereby reducing the drag. Again Jones was correct in this assessment and he pursued the matter in more detail later in his career.

Appendix 4

Supermarine Schneider Trophy Seaplanes & Type 224

Mitchell's sleekly streamlined Supermarine S4 with its unbraced monoplane wing was seen as a game-changer in the Schneider Trophy contests. Its design was all the more astonishing since it came from a designer previously wedded to heavily-braced biplane layouts. Its crash at Chesapeake Bay in October 1925, which the pilot luckily survived, was suspected as being due to the wing's aeroelastic instability. Consequently, Mitchell's subsequent Schneider Trophy contenders featured wire-braced monoplane wings. A further change involved the means by which engine cooling was achieved. According to Bazzocchi⁽⁵²⁾, Mitchell calculated that 38% of the S4's drag came from the aircraft's underwing Lamblin radiators, the probable cause of the very high C_{D0} value given below. Subsequent Supermarine contenders used double skins on the floats, the coolant being pumped through the gap between the skins and thereby eliminating cooling drag.

Taking up Jones's suggestion⁽¹⁸⁾, estimates are made here for the C_{D0} values of all of the Supermarine Schneider Trophy contenders and that for the Supermarine Type 224, the forerunner of the Spitfire. The floatplane data are taken from Andrews and Morgan⁽⁵³⁾, data with which James⁽⁵⁴⁾ largely agrees. These data had appeared in an earlier article by Andrews and Cox⁽⁵⁵⁾ in which it is stated that the dimensional and speed data are "From official and company records. Any variations from figures sometimes published are due to differential loadings for test flight series". Engine data are stated to be "From Napier and Rolls-Royce records". However, the Andrews and Morgan⁽⁵³⁾ data for the S6B list two maximum speeds, 390 mph and 407.5 mph, but only one power value of 2350 hp. In contrast, James⁽⁵⁴⁾ notes that the higher speed achieved by the S6B for the World Speed Record of 407.5 mph was produced using a higher-powered 'Sprint' version of the Rolls-Royce R engine of "some 2600 hp". Bazzocchi⁽⁵²⁾ is more specific, giving the value of 2650 hp and it is this which is used here.

One assumption made in the calculation of C_D using equation (A2.2) is that the performance data for engine power and maximum speed are for straight and level flight at close to sea level conditions. Sea level air density is taken from the International Standard Atmosphere (ISA) tables (see, for example, Reference 37). As to propeller efficiency η , the values assumed are those provided by Bazzocchi⁽⁵²⁾ for the S5 and S6B, the value for the latter being applied to the S6. For the S4, η is taken to be 0.8, a value which is also used for the Type 224. In the calculation of C_{D0} the values of C_{Di} emerge as being very small, ranging from 5×10^{-4} to 8×10^{-4} .

The C_{D0} results are shown in Table 11A, those for the S6 and S6B being gratifyingly consistent for aircraft which are, aerodynamically, almost identical. The result for the S4 is exceptionally high, 0.048, and, as noted above, probably due to its radiator system. In contrast, Loftin⁽⁵⁾ produces a much lower value of 0.027 but this is based on a reduced engine power, 450 hp, which appears erroneous. Bazzocchi⁽⁵²⁾ has given numerical results for C_{D0} for the S4, S5 and S6 and these are listed in Table 11B, together with his assumed engine powers. His result for the S4 is close to that calculated here and must surely have been based on the speed listed in Table 11A, this having the official status of a World Seaplane Record. The difference in C_{D0} , around 2%, might be due to a different value selected for η (unstated) and his choice of an air density value other than that of the ISA. His

result for the S5 is more problematic since, with a lower power, he obtains a higher C_{D0} value. The cause of this might, in part, be due to his choice of a maximum speed different to that given in Table 11A. In this respect, it should be noted that C_D is very sensitive to the value of the speed selected. The $P \sim V^3$ form of equation (A2.2) indicates that slight differences in speed are magnified roughly by a factor of three in C_D calculations. To illustrate this, the calculation procedure has been reversed for Bazzocchi's S5 data. His power and C_{D0} data in Table 11B are used to estimate the maximum speed, listed there as 306 mph. This drop of roughly 4% in speed compared with that listed in Table 11A results in roughly a 10% change in C_{D0} . A similar problem appears in the case of Bazzocchi's S6 data, for which the speed given in Table 11A is again a World Speed Record which one would expect Bazzocchi⁽⁵²⁾ to use. If, however, he did not, the result of the reverse calculation yields the speed of 345 mph listed in Table 11B, a drop of around 3.6% which leads to the 10% change in C_{D0} .

Despite the questionable accuracy of the C_{D0} results in the two Tables, their values are all high compared with later monoplanes but are the inevitable consequence of the 'fixed undercarriage' layout adopted. The floats necessary to their mission requirements, however well-streamlined, inevitably create significant parasite drag.

Table 11A Characteristics of Supermarine Schneider Trophy and Type 224 Aircraft

	S4 (1925)	S5 (1927)	S6 (1929)	S6B (1931)	S6B* (1931)	Type 224 (1934)
Power (hp)	680	900	1,900	2,350	2,650	600
Span (ft)	30.58	26.75	30	30	30	45.83
Wing Area S (ft ²)	139	115	145	145	145	295
Weight (lbs)	3,191	3,242	5,771	6,086	6,086	4,743
Prop. Efficiency η	0.8	0.814	0.84	0.84	0.84	0.8
Speed (mph)	226.75**	319.27	357.7**	390	407.5**	228
Aspect Ratio, A	6.73	6.22	6.21	6.21	6.21	7.12
C_{D0}	0.048	0.028	0.033	0.033	0.033	0.030

* World Speed Record S6B with 'Sprint' R engine of higher power.

** World Speed Record

Table 11B Bazzocchi's Results, Reference 52

	S4	S5	S6	S6B
Power (hp)	680	875	1,900	2,650
C_{D0}	0.049	0.031	0.037	?
Speed (mph)	226.75**	306	345	407.5**

The Type 224 data included in Table 11A have been obtained from Andrews and Morgan⁽⁵²⁾ and Morgan and Shacklady⁽³⁴⁾ which suggest that the aircraft achieved a maximum speed of 228 mph at an altitude of 15,000 ft when powered by a Goshawk engine of 600 hp. The value of C_{D0} based on these data, the air density at altitude being taken from the ISA table, is

included in Table 11A. It is seen to be high, a result of such drag-enhancing features as its large wing of high thickness-chord ratio, open cockpit and fixed, trousered undercarriage. As described in Reference 2, it was the Supermarine team's dissatisfaction with this aircraft's high drag which led to the complete redesign resulting in the Spitfire.

The C_{D0} calculations given here are all rather tentative. All that can be claimed for them is that, having taken the initial data at face value and obeyed the stated assumptions, the listed C_{D0} results follow. Readers in possession of more accurate data for any of these aircraft are encouraged to communicate them via, perhaps, the Correspondence column of this Journal.

Appendix 5

The Heinkel He. 70 & The RAE's Assessment

The Heinkel He. 70 first flew in December 1932 and its high speed performance rapidly attracted considerable interest. In 1933 Ernst Heinkel's report ⁽⁵⁶⁾ on the aircraft provided performance data obtained from flight tests by the Deutsche Versuchsanstalt für Luftfahrt (DVL) together with much detail on its design, structure and aerodynamic features. In the following year the NACA produced an English translation of Heinkel's report (see Reference 56).

To illustrate the aircraft's superior aerodynamic quality, Heinkel ⁽⁵⁶⁾ used a version of the $P \sim V^3$ relation (A2.2) which introduced what he called the 'high-speed index'. This is η/C_D and from equation (A2.2) it follows that at sea-level conditions

$$\eta/C_D = \frac{1}{2} \rho_0 V^3 S/P. \quad (\text{A5.1})$$

For a given aircraft the values of wing planform area, S , and engine power, P , are known and its maximum speed, V , has been obtained from flight tests. At sea level, the air's density is ρ_0 . Consequently all the terms on the right hand side of equation (A5.1) are known and that relation yields a value for the combination η/C_D but not its individual constituents' values which remain unknown. Nonetheless, the aim is to produce the highest possible value for this index since this implies not merely a high value for propeller efficiency η but, more importantly, a low value for the drag coefficient C_D . Heinkel ⁽⁵⁶⁾ provides values of η/C_D for a number of recent American aircraft which have led the field in speed performance and those for the Northrop Alpha and the Lockheed Orion are listed in Table 12. Heinkel ⁽⁵⁶⁾ points with approval to the retractable undercarriage on the Orion together with the cowling for its radial engine. He admits that, until recently, German attempts to compete with the Orion have been unsuccessful, citing the Junkers Ju. 60 (Table 12) as an example. However, he stresses that this situation has changed markedly with the advent of the He. 70, as Table 12 shows.

Table 12 Drag of a number of aircraft

	'High-speed Index' η/C_D
Northrop Alpha (1930)	25.3
Lockheed Orion (1931)	35.6
Junkers Ju. 60 (1932)	26.1
Heinkel He. 70 (1932)	52.8

Source: Heinkel, Reference 56

The values of η/C_D listed in Table 12 are consistent with the data for C_{D0} given in Tables 1 and 2 if account is taken of the fact that, due to induced drag, C_D is slightly greater than the Table 12 C_{D0} values and the propeller efficiencies are taken to lie in the region 0.75 – 0.80. Performance data for various versions of the Heinkel He. 70 will be given later.

As to the choice of aerodynamic shape, Heinkel ⁽⁵⁶⁾ states that no wind tunnel tests were made to aid in this. He favours an elliptic planform wing of aspect ratio 6 but makes no mention of the fact that this choice minimizes induced drag. However, as indicated in Section 2, induced drag is small at high speed and minimizing it is of minor benefit. Heinkel ⁽⁵⁶⁾ favours this shape since it provides a broad chord inboard, offering ample room for the main undercarriage's outward retraction. As related in Reference 2, Mitchell had a similar reason for his choice of this shape in the Spitfire's design. As to thickness-chord ratio, Heinkel ⁽⁵⁶⁾ states that this is 17.5% at the wing root but tapers considerably toward the tip. The emphasis in the design, Heinkel ⁽⁵⁶⁾ stresses, is in the reduction of parasite drag. Thus the undercarriage, including the tail skid, is fully retractable. So too is the radiator for the twelve-cylinder BMW engine using ethylene glycol as coolant (see Condition A in Figure 16). Use of the latter also allows the radiator matrix to be smaller both in size and weight, thus producing less drag when the radiator is deployed.

A further drag-reducing feature, Heinkel ⁽⁵⁶⁾ notes, lies in the geometry of the wing root attachment to the circular-section fuselage. For this low wing design, the wing root abuts the fuselage square to its surface. This creates anhedral for the wing in the immediate vicinity of its root but a short distance outboard this turns to slight dihedral so as to provide lateral stability. Heinkel ⁽⁵⁶⁾ states that the maximum speed was increased slightly after wing root fillets were added. He adds that items contributing parasite drag are designed to minimize this effect; door knobs and foot-steps are inset and the windows are flush-mounted. Finally, the wings, fuselage and control surfaces are shell-plated and flush-riveted.

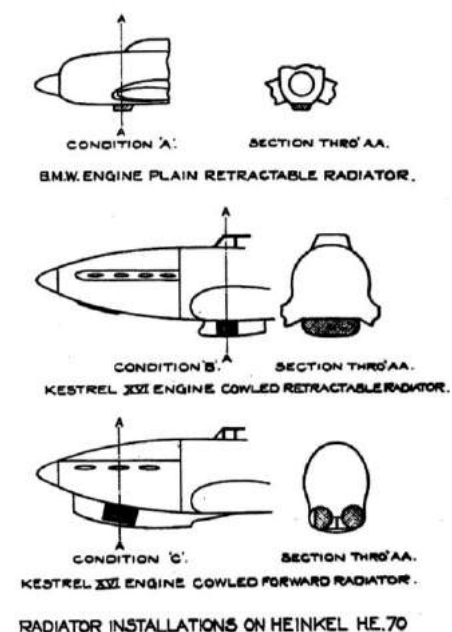


Figure 16 Heinkel He. 70 radiators, Source: Hufton, Reference 59

Such was the British interest in the He. 70 that Vickers constructed a 1/18th scale model of it which was tested in the company's wind tunnel in order to measure its drag coefficient. Subsequently the model was tested at the RAE and then transferred to the National Physical Laboratory for testing at higher Reynolds numbers in the Compressed Air Tunnel (CAT). The CAT results, together with those obtained by Vickers and the RAE, appeared in an ARC report by Jones and Smyth⁽⁵⁷⁾ dated February 1936. It was estimated that at its maximum speed the He. 70 flew at a C_L value of 0.116 and the CAT tests were therefore carried out at that value. Both the Vickers and the RAE tests had been conducted at the slightly higher C_L value of 0.136 and their C_D results lay slightly above those from the CAT, in part due to the effect of higher induced drag. However, once induced drag had been deducted, Jones and Smyth⁽⁵⁷⁾ conclude that at the CAT's highest test Reynolds number, Re , of 5.6×10^6 , obtained with the tunnel running at 24 atmospheres pressure, the value of C_{D0} is 0.0151. This extrapolates well to the full-scale aircraft's similar C_{D0} value deduced from DVL data given by Heinkel⁽⁵⁶⁾ at the even higher Re value of 1.8×10^7 . As to the model's C_{D0} variation with Re , this is plotted in terms of the related coefficient C_f and it is this variation which is included in Section 5's Figure 5 taken from Reference 23. As mentioned in Section 5, $C_f = S C_{D0} / E$, E being the aircraft's total wetted area and S the wing planform area. The Vickers estimate for the He. 70's total wetted area E is 1230 ft² and S is 393 ft² so that for both the model and the full-scale aircraft $E/S = 3.13$. This happens to be close to the average value chosen by Jones⁽¹⁸⁾, $E/S = 3.2$ (see Appendix 3), in calculating his theoretical performance curves shown in Figure 4.

Rolls-Royce took delivery of its Kestrel-powered He. 70, G-ADZF, in March 1936 shortly after the first flight of the Spitfire. As tested by the DVL, the early version of the He. 70 had a retractable radiator which dropped baldly into the airstream with no surrounding cowl to create further drag (Figure 16's Condition A). G-ADZF had a forward radiator enclosed within a fixed cowl designed by Rolls-Royce in which the radiator itself did not fully retract (Figure 16's Condition C). The airflow was straight-through, the cowl providing no entry flow divergence as advocated by Meredith⁽²⁶⁾ to reduce the radiator matrix's drag. G-ADZF also had a fixed tail skid, unlike the earlier He. 70.

After flight testing at Rolls-Royce's Hucknall site a few miles north of Nottingham, the aircraft was transferred to the RAE for assessment, the cowled radiator now moved back to a ventral position (Figure 16's Condition B). A short RAE report by Hufton and Smith⁽⁵⁸⁾, dated January 1937, outlines the test procedures adopted and gives preliminary results. Initially the position error of the aircraft's Pitot-static head was determined for high speeds by a series of flights over a speed course seven miles long at a height of 2,000 ft using timing from the aircraft; at low speeds a suspended static head was used. The conclusion was that, with the radiator retracted as far as possible, the maximum speed was 258 mph at 14,500 ft altitude, but that this was reduced by 10 mph with the radiator fully deployed within the cowl. The rest of the report⁽⁵⁸⁾ is concerned with rate of climb measurements. A later report, it was stated, would analyse the speed results.

This analysis is contained in Hufton's report⁽⁵⁹⁾ of May 1937 in which he compares C_{D0} and other data obtained from the maximum speed results of the DVL, Hucknall and RAE tests. In

particular, these data were used to determine the cleanness ratios for the three radiator configurations examined. However, cleanness ratios are here still based on flat plate turbulent boundary-layer data and are therefore of rather dubious accuracy. The results are listed in Table 13. The values for the propeller efficiency η seem rather high compared with those used later by Hufton⁽³³⁾. The values for gross wing area and wetted area differ slightly since in analysing the DVL tests the values were the best that could be obtained from rather crude drawings. At the RAE the dimensions of the actual aircraft were measured; the difference, Hufton⁽⁵⁹⁾ explains, is partly a genuine one due to differences in the wing root fillets and tailplanes. Table 13's C_{D0} and CR values for the Hucknall tests are those listed in Table 2 of Section 5 drawn from Reference 22.

Table 13 Heinkel He. 70 characteristics

	DVL	RAE	Hucknall
Engine	BMW	Kestrel XVI	Kestrel XVI
Radiator	Plain retractable	Cowled retractable	Forward cowled
Gross Wing Area, S, ft ²	393	390	390
Wetted Area, E, ft ²		1237	1305
Maximum Speed, mph	235	219	239
Altitude, ft	0	1900	3000
Power, hp	660	599	662
Propeller Efficiency, η	0.800	0.814	0.822
C_L	0.134	0.164	0.132
C_D	0.0154	0.01825	0.0159
C_{Di}	0.00095	0.00141	0.000915
C_{D0}	0.0144		0.01685
Cleanness Ratio, CR	0.559	0.479	0.544
Total Drag @ 100 ft/s, lbs	72	84.5	74
Tail Skid Estimate, lbs	0	4	4
C_{D0} (No Tail Skid)	0.0144	0.01605	0.0142
CR (No Tail Skid)	0.559	0.518	0.575

Source: Hufton, Reference 59

The last four lines of Table 13 indicate Hufton's interest in estimating the drag improvement if the tail skid is made retractable. Morgan⁽²⁵⁾, in assessing the He. 70, comments that "the tail skid was of a rather clumsy design" and assigns to it 4 lbs in drag, as does Hufton⁽⁵⁹⁾.

The next step in the RAE's assessment of the He. 70 entailed testing it in the 24 ft Open Jet

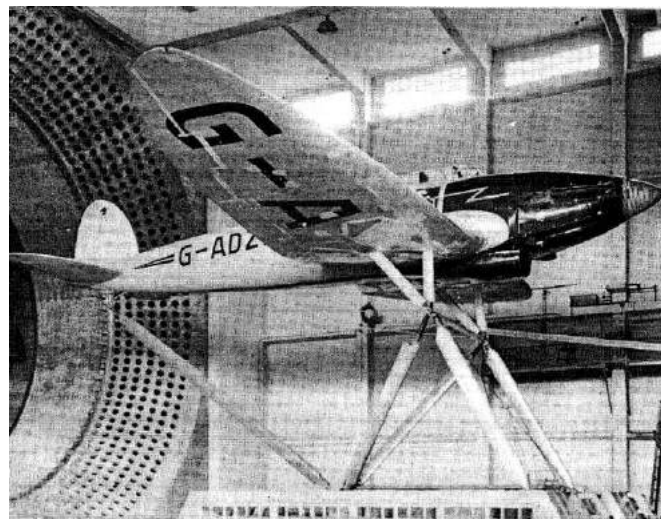


Figure 17 Heinkel He. 70 in the RAE 24 ft Open Jet Tunnel. Source Farnborough Air Sciences Trust.

Tunnel, a facility which had begun operation in 1935 (Figure 17). The results are given in the report by Shaw and Diprose⁽⁶⁰⁾ dated December 1937. Since the He. 70's wing span is slightly above 48 ft, some 12 ft of the outboard part of each wing projected beyond the tunnel's jet. However, a correction based on the known C_{D0} for the aerofoil section was applied in an attempt to deal with this difficulty. The report⁽⁶⁰⁾ takes the view that this "did not detract much from the value of the tests since the investigation was mostly concerned with the wing root, fuselage and engine details where it was felt that there was most chance of effecting improvements". The report⁽⁶⁰⁾ proposes that similar tests be made on other high speed aircraft when they become available. The later Hurricane tests mentioned by Collar⁽²⁴⁾ indicate that this advice was followed.

The investigation⁽⁶⁰⁾ included drag measurements made with the ventral radiator, with the nose radiator, after leaks had been sealed and after excrescences had been removed. Pitot-static traverses were carried out in the fuselage boundary layer aft of the cabin hood and aft of the wing root. Also wool tufts were used to investigate the flow around the entries to the cowled radiators.

For the tests the tail skid was removed, as was the propeller which was replaced by a spinner. In the investigation of leaks, sealing was effected with linen tape and adhesive. Shaw and Diprose⁽⁶⁰⁾ note that the He. 70 is comparatively free of the seams and removable panels which are common leak sources on most military aircraft. So although leaks on this aircraft amounted to only about 8% of the total drag, they felt that the exercise clearly pointed to the importance of attempting to reduce leakage on more leak-prone military aircraft. In the investigation of parasite drag, excrescences such as exhaust pipes and air intakes were removed whereas small pipes and knobs which could not be removed were faired.

The drag reductions produced for the case in which the cowled radiator was sited at the nose are listed in Table 14. The initial total drag, 88.7 lbs, is significantly higher than that listed in Table 13, 74 lbs, which was deduced by Hufton⁽⁵⁹⁾ from flight test data. This Shaw and Diprose⁽⁶⁰⁾ largely attribute to the difference in Reynolds number Re between the two cases, the Re value achieved in the Open Jet Tunnel being 0.4 of that reached at maximum speed in

Table 14 Heinkel He. 70 in 24 ft tunnel, Drag & Drag Reductions in lbs at 100 ft/s

	Drag & drag reduction in lbs at 100 ft/s
Drag with nose radiator*	88.7
Leak sealing reduction	7.1
Removing nose radiator**	5.2
Removing tail skid	4.0
Removing exhausts, air intakes etc.	2.2
Drag completely faired	70.2

* Includes 13.3 lbs added for wings outside jet.

** Removing ventral radiator 7.3 lbs from total of 90.8 lbs.

Source: Shaw and Diprose, Reference 60

flight. As evidence for this, they point to the decrease in drag coefficient with increasing Re shown by flat plate data; Figures 5 and 14 and equation (8) illustrate this behaviour. The more accurate but yet to be announced Squire and Young⁽²⁹⁾ analysis shows a similar decreasing drag with increasing Re but the drag is higher than that for the flat plate due, for example, to the additional boundary-layer pressure drag (see equation (11)). Parasitic items having bluff shapes causing local separation, on the other hand, can show little variation over wide ranges of Re . With this uncertainty concerning Re behaviour, the value of the data listed in Table 14 therefore lies mainly in the scale of the drags revealed for individual parasitic items. In contrast, the initial and final drags, 88.7 lbs and 70.2 lbs, seem of rather dubious accuracy considering the rather simplistic estimate of 13.3 lbs for the drag addition due to the wings projecting beyond the tunnel's jet. Although Shaw and Diprose⁽⁶⁰⁾ do not do so, calculation of C_{D0} based on the above drag for the aircraft before modification yields the value 0.0191 whereas for the completely faired aircraft it is 0.0151.

The Pitot-static traverse method used by Shaw and Diprose⁽⁶⁰⁾ had emerged in 1936 from an earlier analysis by B. M. Jones supported by experimental work, both in flight and in a wind tunnel, at Cambridge University⁽⁶¹⁾. One of the participants in the wind tunnel tests was Flight Lieutenant Frank Whittle, then a Cambridge student. Another such was Alec Young, who later brought his understanding gained from this link between an aerofoil's trailing-edge flow and its wake to the turbulent boundary-layer analysis of Squire and Young⁽²⁹⁾. Shaw and Diprose⁽⁶⁰⁾ carried out their Pitot-static traverses at a distance of 20 ft aft of the He. 70's nose, in one case a little aft of the fuselage's cabin hood, in the other slightly aft of the wing root. In the latter tests they could detect no sign of wing-fuselage interference. This they attributed to the beneficial effects of the wing root anhedral and fillets, as Heinkel⁽⁵⁶⁾ had suggested. The fuselage traverses aft of the cabin hood yielded a drag higher than that anticipated from flat plate turbulent boundary-layer data. This Shaw and Diprose⁽⁶⁰⁾ attributed to the effect of the cabin hood.

The use of wool tufts in the Open Jet Tunnel tests revealed flow separation around the radiator cowl's entry. Shaw and Diprose⁽⁶⁰⁾ suggested that this could be rectified by keeping the entry clear of the fuselage boundary layer. As mentioned in Reference 2, it seems this measure was suggested to the Mustang's design team by Beverley Shenstone, previously Mitchell's aerodynamicist for the Spitfire design, although it may not necessarily be the case that this advice sprang from the He. 70 tests in the Open Jet Tunnel.

Meanwhile Hufton had been attempting a more detailed analysis of the flight test data obtained with G-ADZF. These data now included results for the aircraft fitted with a new radiator arrangement in which a redesigned and slightly larger cowled forward unit used water as the coolant. His report⁽⁶²⁾, appearing in May 1938, is largely concerned with the effects of different radiator deployments together with reassessments of propeller efficiency and engine power variation with altitude. From this Hufton⁽⁶²⁾ concludes that there is no variation of L/D with altitude due to Reynolds number variation and the maximum value of L/D is 15.8 at $C_L = 0.46$.

One consequence of this re-appraisal is that his earlier C_D values are now increased. These cover a range of radiator flap settings and also three radiator deployments: fully retracted, partially retracted and fully exposed. These C_D values have been obtained at various C_L values and therefore at different speeds and thus different Reynolds numbers. In estimating C_{Di} , which is deducted from C_D so as to give C_{D0} , Hufton⁽⁶²⁾ uses equation (5) with $k = 1$, an adequate approximation since C_{Di} is generally small at high speed. His C_{D0} values range from 0.0156 to 0.0191, depending on these various radiator settings and deployments. The best result, $C_{D0} = 0.0156$, is for the nose glycol radiator described as in a level condition, the worst case being $C_{D0} = 0.0191$ with the ventral glycol radiator deployed and its flap down. If nothing else, though, these results illustrate the importance of radiator design in controlling drag. However, one puzzling aspect of the results is that the various C_{D0} values calculated appear to depend on the C_L conditions from which they were obtained. Here one is reminded of Courtney's dictum⁽⁴³⁾ that drag estimation is by no means an exact science. Indeed, this situation is similar to that later encountered by Courtney⁽⁴³⁾ (see Section 6) in which Reynolds number variation helped to explain such curious behaviour. It would be interesting to try his procedure in which a graph of $C_D \sim C_L^2$ is plotted to estimate C_{D0} and k . Regrettably, there being so many different radiator conditions investigated, too few data points at any one condition are available to make this procedure viable.

Hufton⁽⁶²⁾ ends the summary of his main conclusions with the cryptic statement "No further work is proceeding". It was time to turn away from the He. 70 and move to the more urgent assessments of the new military aircraft coming into service. Nonetheless, the RAE had learned much from its detailed investigation of this extraordinarily low drag aircraft.

Dr J A D Ackroyd CEng FRAeS

Born in Bradford, Yorkshire, in 1938, John Ackroyd graduated in Aeronautical Engineering in 1960 at Queen Mary College, University of London. After doctoral and postdoctoral research in shock tubes there, he joined the staff of the Department of the Mechanics of Fluids (later the Aerospace Division, Manchester School of Engineering) of the Victoria University of Manchester. He taught in aerodynamics, flight dynamics, aircraft structures and propulsion whilst carrying out research in boundary-layer theory. He retired in 2000 as Senior Lecturer. His interest in the technical history of aviation resulted in him giving the Royal Aeronautical Society's Lanchester (1991) and Cayley (2000) Lectures, the Inaugural Cody Lecture (2003) and the Cody Lecture (2015). Together with B. P. Axcell and A. I. Ruban, he is co-author of *Early Developments of Modern Aerodynamics* published jointly by the AIAA and Butterworth-Heinemann (now Elsevier) in 2001.